Inorg. Chem. **2002**, *41*, 1502–1517

Characteristics and Properties of Metal-to-Ligand Charge-Transfer Excited States in 2,3-Bis(2-pyridyl)pyrazine and 2,2′-Bypyridine Ruthenium Complexes. Perturbation-Theory-Based Correlations of Optical Absorption and Emission Parameters with Electrochemistry and Thermal Kinetics and Related Ab Initio Calculations

Dhehinie S. Seneviratne, Md. Jamal Uddin, V. Swayambunathan, H. Bernhard Schlegel, and John F. Endicott*

Department of Chemistry, Wayne State University, Detroit, Michigan 48202-3815

Received February 9, 2001

The absorption, emission, and infrared spectra, metal (Ru) and ligand (PP) half-wave potentials, and ab initio calculations on the ligands (PP) are compared for several $[L_nRu(PP)]^{2+}$ and $[\{L_nRu\}dpp\{RuL'_n\}]^{4+}$ complexes, where L_n and L'_n = $(bpy)_2$ or $(NH_3)_4$ and PP = 2,2′-bipyridine (bpy), 2,3-bis(2-pyridyl)pyrazine (dpp), 2,3-bis(2-pyridyl)quinoxaline (dpq), or 2,3-bis(2pyridyl)benzoquinoxaline (dpb). The energy of the metal-to-ligand charge-transfer (MLCT) absorption maximum ($h\nu_{max}$) varies in nearly direct proportion to the difference between Ru^{III}/Ru^{II} and $(PP)/(PP)^-$ half-wave potentials, $\Delta E_{1/2}$, for the monometallic complexes but not for the bimetallic complexes. The MLCT spectra of $[(NH_3)_4Ru(dpp)]^{2+}$ exhibit three prominent visible–near-UV absorptions, compared to two for $[(NH_3)_4Ru(bpy)]^{2+}$, and are not easily reconciled with the MLCT spectra of $[\{(NH_3)_4Ru\}dpp\{RuL_n\}]^{4+}$. The ab initio calculations indicate that the two lowest energy π^* orbitals are not much different in energy in the PP ligands (they correlate with the degenerate π^* orbitals of benzene) and that both contribute to the observed MLCT transitions. The LUMO energies calculated for the monometallic complexes correlate strongly with the observed $h\nu_{max}$ (corrected for variations in metal contribution). The LUMO computed for dpp correlates with LUMO + 1 of pyrazine. This inversion of the order of the two lowest energy π^* orbitals is unique to dpp in this series of ligands. Configurational mixing of the ground and MLCT excited states is treated as a small perturbation of the overall energies of the metal complexes, resulting in a contribution ϵ_s to the ground-state energy. The fraction of charge delocalized, α_{DA}^2, is expected to attenuate the reorganizational energy, χ_{reorg}, by a factor of approximately $(1 - 4\alpha_{DA}^2 + \alpha_{DA}^4)$, relative to the limit where there is no charge delocalization. This appears to be a substantial effect for these complexes ($\alpha_{DA}^2 \cong 0.1$ for Ru^{II}/bpy), and it leads to smaller reorganizational energies for emission than for absorption. Reorganizational energies are inferred from the bandwidths found in Gaussian analyses of the emission and/or absorption spectra. Exchange energies are estimated from the Stokes shifts combined with perturbation--theory-based relationship between the reorganizational energies for absorption and emission values. The results indicate that ϵ_s is dominated by terms that contribute to electron delocalization between metal and PP ligand. This inference is supported by the large shifts in the N–H stretching frequency of coordinated NH_3 as the number of PP ligands is increased. The measured properties of the bpy and dpp ligands seem to be very similar, but electron delocalization appears to be slightly larger (10–40%) and the exchange energy contributions appear to be comparable (e.g., $\sim 1.7 \times 10^3$ cm^{-1} in $[Ru(bpy)_2dpp]^{2+}$ compared to $\sim 1.3 \times 10^3$ cm^{-1} in the bpy analogue).

Introduction

There has been a great deal of interest in the properties of covalently linked, polymetallic transition metal complexes. These compounds can often be assembled in supramolecular arrays that might be useful in applications such as the collection of light energy and its transformation into chemically useful forms, the conduction of charge in molecular level devices, and other unique chemical properties.[1−4] One

* To whom correspondence should be addressed. E-mail: jfe@chem.wayne.edu.

10.1021/ic010172c CCC: $22.00
Published on Web 02/27/2002

of the simplest linkers commonly used in assembling metals into such arrays is 2,3-bis(2-pyridyl)pyrazine (dpp).[5−18] This molecule can function as a bidentate ligand to two metals simultaneously, and the relatively low-energy LUMO of the pyrazine moiety is expected to facilitate electronic delocalization between the bridged metals.[19−22] Partly for these reasons, we began some systematic studies of dpp-bridged complexes several years ago.[23] At that time we also thought that such polypyridyl types of bridging ligands might exhibit some of the features characteristic of the mixing of bridging ligand nuclear properties with donor−acceptor (D/A) electronic properties that have been found for cyanide-bridged donors and acceptors[24−30] and, if not similar, that their properties could provide an instructive contrast between different classes of strongly coupled transition metal donor−acceptor complexes. As our work has progressed, it has become evident that complexes with dpp ligands have some unexpected spectroscopic and chemical properties. Related features have been noted in earlier work. For example, several research groups have noted that the bidentate coordination of two metals by dpp results in some twisting of the pyrazine ring.[6,11,13,15] It has also been observed that the electrochemical properties of the dpp-bridged complexes do not correlate with bond order in the same manner as those of related complexes;[9] in order to fit the bond order correlation, bonds of the pyridine moieties had to be included for dpp but not for closely related ligands.

The difference in the electrochemical potential for oxidation of the donor (Ru^{II} in systems reported here) and the potential for reduction of a linked acceptor ligand (e.g., a polypyridyl ligand) commonly correlates strongly with the lowest energy MLCT absorption maximum as in eq 1,[31−36]

$$h\nu_{max}(\mathrm{MLCT}) = F[E_{1/2}(D^{+}|D) - E_{1/2}(A|A^{-})] + \eta_{DA} = F\,\Delta E_{1/2}(D/A) + \eta_{DA} \quad (1)$$

where F is Faraday's constant and the potentials are determined in the assembled complex.[31,32] In the experimental correlations of monometallic complexes, the η_{DA} cross term has been commonly found to be small, $\sim(0-2) \times 10^3$ cm^{-1}, for polypyridine acceptors.[31,33−35] In contrast, η_{DA} has been found to be $\sim 5 \times 10^3$ cm^{-1} for some pyrazine-bridged bimetallic complexes.[37] The general success of eq 1 has led to the proposal that $h\nu_{max}$(MLCT) can be represented as the sum of independent contributions of the donor, $F(D)^o$, and the acceptor, $F(A)^o$, with a small correction for cross terms, Γ_{DA}, as in eq 2.[31]

$$h\nu_{max}(\mathrm{MLCT}) = F(D)^o + F(A)^o + \Gamma_{DA} \quad (2)$$

In the limit that the donor−acceptor coupling is very small ($H_{DA}/E_{DA} \rightarrow 0$, where H_{DA} is the electronic matrix element and E_{DA} is the energy difference between the ground and excited state evaluated in the nuclear coordinates of the ground-state PE minimum), the physical significance of the $F(D)^o$, $F(A)^o$, and Γ_{DA} terms is relatively simple[38] (see the Discussion; note that $F(D)^o$ and $F(A)^o$ contain reorganizational free energy as well as electrochemical contributions). The physical significance of the Γ_{DA} and η_{DA} terms is clear when D/A electronic coupling is weak ($H_{DA} < 200$ cm^{-1}) but not in the strongly coupled limit typical of ruthenium−polypyridine complexes. We have employed the simple

(1) Balzani, V., Scandola, F., Eds. *Supramolecular Photochemistry*; Horwood: Chichester, U.K., 1991.
(2) Atwood, J. L., Davies, J. E. D., MacNicol, D. D., Vogtle, F., Eds.; *Comprehensive Supramolecular Chemistry*; Pergamon: Oxford, U.K., 1996.
(3) Meyer, G. J., Ed. *Molecular Level Artificial Photosynthetic Materials*; Wiley: New York, 1997.
(4) Brewer, K. J. *Comments Inorg. Chem.* **1999**, *21*, 201.
(5) Braunstein, C. H.; Baker, A. D.; Strekas, T. C.; Gafney, H. D. *Inorg. Chem.* **1984**, *23*, 857.
(6) Rillema, D. P.; Taghdiri, D. G.; Jones, D. S.; Keller, C. D.; Word, L. A.; Meyer, T. J.; Levy, H. *Inorg. Chem.* **1987**, *26*, 578.
(7) Ruminiski, K. K.; Cockcroft, T.; Shoup, M. *Inorg. Chem.* **1988**, *27*, 4026.
(8) Murphy, R. W., Jr.; Brewer, K. J.; Gettliffe, G.; Petersen, J. D. *Inorg. Chem.* **1989**, *28*, 81.
(9) Cooper, J. B.; MacQueen, D. B.; Petersen, J. D.; Wertz, D. W. *Inorg. Chem.* **1990**, *29*, 3701.
(10) *J. Phys. Chem.* **1992**, *96*, 5865.
(11) Kirchoff, J. R.; Kirschbaum, K. *Polyhedron* **1998**, *17*, 4033.
(12) Denti, G.; Campagna, S.; Sabatino, L.; Seroni, S.; Ciano, M.; Balzani, V. *Inorg. Chem.* **1990**, *29*, 4750.
(13) Marcaccio, M.; Poalucci, F.; Paradisi, C.; Roffia, S.; Fontanesi, C.; Yellowlees, L. J.; Serroni, S.; Campagna, S.; Denti, G.; Balzani, V. *J. Am. Chem. Soc.* **1999**, *121*, 10081.
(14) Serroni, S.; Juris, A.; Campagna, S.; Venturi, M.; Denti, G.; Balzani, V. *J. Am. Chem. Soc.* **1994**, *116*, 9086.
(15) Scott, S. M.; Gordon, K. C.; Burrell, A. K. *J. Chem. Soc., Dalton Trans.* **1999**, 2669.
(16) Sauvage, J.-P.; Collin, J.-P.; Chambron, J.-C.; Guillerez, S.; Coudret, C. *Chem. Rev.* **1994**, *94*, 993.
(17) Campagna, S.; Denti, G.; Serroni, S.; Ciano, M.; Balzani, V. *Inorg. Chem.* **1991**, *30*, 3728.
(18) Ceroni, P.; Paolucci, F.; Paradisi, C.; Juris, A.; Roffia, S.; Serroni, S.; Campagna, S.; Bard, A. J. *J. Am. Chem. Soc.* **1998**, *120*, 5480.
(19) Richardson, D. E.; Taube, H. *Coord. Chem. Rev.* **1984**, *60*, 107.
(20) Crutchley, R. *Adv. Inorg. Chem.* **1994**, *41*, 273.
(21) Creutz, C. *Prog. Inorg. Chem.* **1983**, *30*, 1.
(22) Creutz, C.; Sutin, N. *Inorg. Chem.* **1976**, *15*, 496.
(23) Swayambunathan, V.; Endicott, J. F. *Abstracts of Papers*, 208th National Meeting of the American Chemical Society; American Chemical Society: Washington, DC, 1994; INOR 229.
(24) Watzky, M. A.; Endicott, J. F.; Song, X.; Lei, Y.; Macatangay, A. V. *Inorg. Chem.* **1996**, *35*, 3463.
(25) Watzky, M. A.; Macatangay, A. V.; Van Camp, R. A.; Mazzetto, S. E.; Song, X.; Endicott, J. F.; Buranda, T. *J. Phys. Chem.* **1997**, *101*, 8441.
(26) Macatangay, A. V.; Song, X.; Endicott, J. F. *J. Phys. Chem.* **1998**, *102*, 7537.
(27) Macatangay, A. V.; Mazzetto, S. E.; Endicott, J. F. *Inorg. Chem.* **1999**, *38*, 5091.
(28) Macatangay, A. V.; Endicott, J. F. *Inorg. Chem.* **2000**, *39*, 437.
(29) Endicott, J. F.; Watzky, M. A.; Macatangay, A. V.; Mazzetto, S. E.; Song, X.; Buranda, T. In *Electron and Ion Transfer in Condensed Media*; Kornyshev, A. A., Tosi, M., Ulstrup, J., Eds.; World Scientific: Singapore, 1997; p 139.
(30) Endicott, J. F.; Watzky, M. A.; Song, X.; Buranda, T. *Coord. Chem. Rev.* **1997**, *159*, 295.
(31) Lever, A. B. P.; Dodsworth, E. In *Electronic Structure and Spectroscopy of Inorganic Compounds*; Lever, A. B. P., Solomon, E. I., Eds.; Wiley: New York, 1999; Vol. II, p 227.
(32) Gorelsky, S. I.; Kotov, V. Y.; Lever, A. B. P. *Inorg. Chem.* **1998**, *37*, 4584.
(33) Curtis, J. C.; Sullivan, B. P.; Meyer, T. J. *Inorg. Chem.* **1983**, *22*, 224.
(34) Timpson, C. J.; Bignozzi, C. A.; Sullivan, B. P.; Kober, E. M.; Meyer, T. J. *J. Phys. Chem.* **1996**, *100*, 2915.
(35) Ohsawa, K. W.; Hanck, K. W.; DeArmond, M. K. *J. Electroanal. Chem.* **1984**, *175*, 229.
(36) Lu, S.; Strelets, V. V.; Ryan, M. F.; Pietro, W. J.; Lever, A. B. P. *Inorg. Chem.* **1996**, *35*, 1013.
(37) Demadis, K. D.; Neyhart, G. A.; Kober, E. M.; White, A. H.; Meyer, T. J. *Inorg. Chem.* **1999**, *38*, 5948.
(38) Endicott, J. F. In *Electron Transfer in Chemistry*; Balzani, V., Ed.; Wiley-VCH: New York, 2001; Vol. 1, p 238.

relations among Γ_{DA}, η_{DA}, energy gaps, and the nuclear reorganizational parameters[31,38−40] in the weakly coupled limit to aid in the evaluation of the more complicated systems. The deviations from this limit can be expressed in terms of a perturbation theory parameter, α_{DA}^2 ($\alpha_{DA} = H_{DA}/E_{DA}$), which can be interpreted as the fraction of electron density delocalized. For example, the absorption bandwidth in the weakly coupled, two-state limit is proportional to the square root of the electron-transfer reorganizational energy,[39,41] but in strongly coupled systems the bandwidth should decrease with α_{DA}^2,[21,39,41−44] as succinctly expressed in eq 3,[44]

$$\lambda_{reorg} \cong \lambda_{reorg}^{o}(1 - 4\alpha_{DA}^{2}) \qquad (3)$$

where λ_{reorg}^{o} is the reorganizational energy defined for the limit of weak coupling.

We initially sought to gain insight into the origin of the complexities of the charge-transfer properties of dpp-containing complexes by means of a careful comparison to the "much better understood" bipyridine complexes.[45] Calculations reported by Lever and Gorelsky[46,47] indicated that there is very little electron delocalization in the bipyridine (bpy) complexes and that large electron exchange energies account for some properties commonly attributed to electon delocalization in these complexes.[48] Since electroabsorption measurements indicate similar extents of metal−ligand mixing in $[Ru(NH_3)_5L]^{2+}$ complexes with L = pyridine and pyrazine,[49] this raised the possibilities (a) that Coulomb and exchange terms may contribute differently to α_{DA} in dpp and bpy complexes and (b) that there is less electron delocalization in the dpp complexes than is generally supposed. The first possibility should lead to some differences in physical properties, and we have found that $[Ru(NH_3)_4dpp]^{2+}$ and some dpp-bridged complexes do have unexpected spectroscopic features. Unfortunately, not all the relevant properties of the bipyridine complexes seem to be as well understood as we had supposed;[50,51] this is illustrated by recent estimates

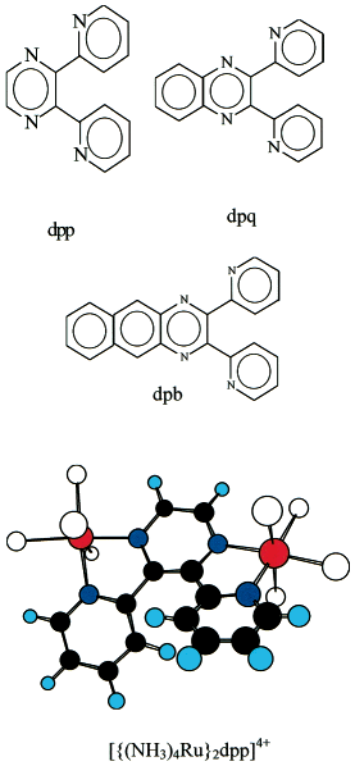

Figure 1. Bridging ligand structures: dpp = 2,3-bis(2-pyridyl)pyrazine; dpq = 2,3-bis(2-pyridyl)quinoxaline; dpb = 2,3-bis(2-pyridyl)benzoquinoxaline. The Chem3D structure at the bottom of the figure illustrates the effect of stereochemical repulsions on the bimetallic structures (at the extended Hückel level with energy minimization).

of 3.9%[31,46,47] and of 25%[52] for the ground-state electron delocalization in $[Ru(NH_3)_4bpy]^{2+}$.

The combination of these experimental issues has led us to perform ab initio computations on dpp and some related ligands. On the basis of the computations and the experimental observations, we propose that some of the unusual spectroscopy and chemistry associated with the dpp ligand may be a consequence of a difference in the nature of the LUMO of dpp from that expected based on pyrazine.

Experimental Section

A. Materials. The ligands (see Figure 1) dpq (2,3-bis(2-pyridyl)-quinoxaline) and dpb (2,3-bis(2-pyridyl)benzoquinoxaline) were synthesized according to literature procedures.[4,53,54] The dpp ligand (2,3-bis(2-pyridyl)pyrazine), NH_4PF_6, KPF_6, and Sephadex C-25 ion-exchange resin were purchased from Aldrich and used without further purification. All solvents used were reagent or spectroscopic grade. Tetrabutylammonium hexafluorophosphate (TBAH) was purchased from Aldrich and dried in a vacuum oven before use. $RuCl_3 \cdot 3H_2O$ was purchased from Strem Chemicals or from Acros and used as received. $Ru(bpy)_2Cl_2 \cdot H_2O$ was purchased from Strem Chemicals and used without further purification.

Preparative solutions were deaerated by passing an argon gas stream through two chromous scrubbers (0.1 M $CrCl_3 \cdot 6H_2O$ in 1 M HCl over Zn/Hg) and then through a $CaSO_4$ column. Distilled water was deionized prior to distillation by passing through two

(39) Hush, N. S. *Electrochim. Acta* **1968**, *13*, 1005.
(40) Endicott, J. F.; Uddin, J. M. *Coord. Chem. Rev.* **2001**, *219−221*, 687.
(41) Hush, N. S. *Prog. Inorg. Chem.* **1968**, *8*, 391.
(42) Cannon, R. D. *Electron Transfer Reactions*; Butterworth: London, 1980.
(43) Marcus, R. A. *J. Phys. Chem.* **1992**, *96*, 1753.
(44) Matyushov, D. V.; Voth, G. A. *J. Phys. Chem. A* **2001**, *104*, 6470.
(45) Seneviratne, D. S. Ph.D. Dissertation, Wayne State University, Detroit, MI, 1999.
(46) Lever, A. B. P.; Gorelsky, S. I. *Coord. Chem. Rev.* **2000**, *208*, 153.
(47) Gorelsky, S. I.; Dodsworth, E. S.; Lever, A. B. P.; Vlcek, A. A. *Coord. Chem. Rev.* **1999**, *174*, 469.
(48) Very recent DFT calculations by Gorelsky and Lever suggest that there is about 10% electron delocalization in the ground state of $[Ru(NH_3)_4bpy]^{2+}$. This calculation also seems to be consistent with the π^* orbital sequence that we have inferred below. Lever, A. B. P.; Gorelsky, S. I. Private communication, October, 23, 2001.
(49) Shin, Y. K.; Brunschwig, B. S.; Creutz, C.; Sutin, N. *J. Phys. Chem.* **1996**, *100*, 8157.
(50) The properties of concern here deal with the amount of electron density delocalized, the absorption and emission bandwidths, the sequence of MLCT excited states, the exchange energy, etc. Our studies of $[Ru(NH_3)_4bpy]^{2+}$ and related complexes are briefly summarized in this report. A preliminary report has been submitted,[51] and a full report is being prepared.
(51) Endicott, J. F.; Schlegel, H. B.; Uddin, J. M.; Seneviratne, D. S. *Coord. Chem. Rev.*, submitted.
(52) Mines, G. A.; Roberts, J. A.; Hupp, J. *Inorg. Chem.* **1992**, *31*, 125.
(53) Goodwin, H. A.; Liona, F. *J. Am. Chem. Soc.* **1959**, *81*, 6415.
(54) Baino, A. J.; Carlson, D. L.; Wolosh, G. M.; DeJesus, D. E.; Knowles, C. F.; Szabo, E. G.; Murphy, W. R. *Inorg. Chem.* **1990**, *29*, 2327.

Mega-Pure organic removal cartridges. Ion exchange chromatography was carried out using gradients of eluant concentrations. Elemental analyses are summarized in Table S1[58] and were performed at Midwest Micro Laboratories (Indianapolis, IN).

B. Synthesis of Compounds. The starting materials $[Ru^{III}(NH_3)_5Cl](Cl)_2$,[55] *cis*-$[(NH_3)_4Ru^{III}Cl_2]Cl$,[56] and $[Ru^{III}(NH_3)_5(O_3SCF_3)_2](O_3SCF_3)$[57] were synthesized according to literature procedures. The following compounds were prepared by slightly modified literature procedures (see pages S2 and S3[58]): (a) $[(bpy)_2Ru(dpp)](PF_6)_2$,[12] (b) $[(bpy)_2Ru\text{-}\mu\text{-}(dpp)Ru(bpy)_2](PF_6)_4$,[12] (c) $[Ru(NH_3)_5(OH_2)](PF_6)_2$,[59] (d) $[Ru(NH_3)_4(dpp)](PF_6)_2$,[7] (e) $[(bpy)_2Ru(dpq)](PF_6)_2$.[12] The skeletal structures of the ligands are shown in Figure 1.

$[(NH_3)_4Ru(dpp)Ru(NH_3)_4](PF_6)_4$. A 0.25 g (0.9 mmol) sample of *cis*-$[(NH_3)_4Ru^{III}Cl_2]Cl$ and a 3-fold molar excess of ligand dpp (0.071 g, 0.3 mmol) were reacted in 20 mL of an argon deaerated ethanol/water mixture in the presence of freshly made Zn/Hg. The reaction was carried out in an argon atmosphere in the absence of light. The yellow reaction mixture was warmed (50 °C) and constantly stirred for 3 h. The blue-violet reaction mixture was filtered, and solid NH_4PF_6 was added until the precipitation was completed. The crude product was isolated after being chilled for 30 min. The crude product was reprecipitated from water. Typical yields were ~40%.

$[(bpy)_2Ru(dpp)Ru(NH_3)_4](PF_6)_4$. A 100 mg (0.11 mmol) sample of $[(bpy)_2Ru(dpp)](PF_6)_2$ was dissolved in 6 mL of argon deareated distilled water. A 38 mg (0.137 mmol) sample of *cis*-$[(NH_3)_4Ru^{III}Cl_2]Cl$ was dissolved separately in 8 mL of argon degassed distilled water and reduced with Zn/Hg for about $^1/_2$ h under argon, wrapped with aluminum foil for protection from light. After this time the reduced ruthenium solution was added to the deaerated $[(bpy)_2Ru(dpp)]^{2+}$ solution. The resulting solution was shielded from light and allowed to react under argon at room temperature for 12 h. The initial brown-orange solution changed to blue-purple during this time. The crude product was isolated as the PF_6^- salt by adding solid NH_4PF_6. The product was purified by ion-exchange chromatography using Sephadex SPC-25 resin and eluted with increasing concentrations of acids. The desired product was eluted with 0.5 M HCl as a blue-purple solution. The solvent was removed by rotary evaporation, and the product was isolated as a chloride salt. Precipitation as the PF_6^- salt gave a very low yield. The typical yield of the chloride salt was about 30%.

$[(NH_3)_4Ru(dpq)](PF_6)_2$. In a typical experiment, a 2-fold excess of dpq ligand (115 mg, 0.4 mmol) and $[(NH_3)_5Ru(OH_2)](PF_6)_2$ (100 mg, 0.2 mmol) were placed in a 50 mL round-bottom flask, which was wrapped with aluminum foil for protection from light. A serum cap was placed on the flask, and the flask was deareated by flushing with argon for 30 min. Deareated acetone (~12 mL) was added by syringe to the flask that contained the two complexes. After 10 min with stirring, the color of the solution changed to blue. The reaction mixture was stirred for 2 h. A constant stream of argon was blown over the solution during this time. After 2 h this solution was added onto stirring anhydrous ether. Care was taken in all procedures to minimize the exposure of either solution or solid samples to light. The product was isolated and purified by reprecipitation from acetone/ether in the absence of light. Typical yield was ~75%. A similar approach was used for the synthesis of $[(NH_3)_4Ru(dpb)](PF_6)_2$.

C. Absorption Spectroscopy. Ultraviolet, visible, and near-infrared spectra were recorded on an OLIS modified Cary 14 spectrophotometer controlled by a Gateway 486/33 PC using OLIS software. UV−visible and near-infrared absorption spectra were recorded in deaerated, distilled water, acetonitrile, and H_2O/DMSO.

The ASCII files of the experimental absorption (or emission) spectra were transferred to EXCEL, and the product of absorption and ν_{abs}[60] was plotted vs ν_{abs} (see eq 6 below). Spectral deconvolutions were then performed using the Grams 32 program.[61] In these fittings of the absorption spectra to Gaussian components, (a) the absorbance was scaled by the frequency as suggested by eq 6, (b) the dominant, lowest energy component was fitted first with a Gaussian closely matched to the maximum energy and the band shape on the low-energy side, (c) higher energy maxima were similarly approximated by Gaussians, (d) a minimum number of minor components was added as needed for a good fit, (e) some properties of at least the major components were fixed (up to two of the maximum energy, intensity and bandwidth) before iteration of the fit, and (f) fixed parameters were removed one at a time as the fit was iteratively refined. Fitting on the high-energy side was always the most difficult and equivocal; the tail of deep-UV absorption bands was approximated by the edge of a Gaussian component. The extended low-energy, low-intensity absorbancies (probably a combination of hot band and triplet contributions) were fit by a small Gaussian component. The parameters for the minor components depended strongly on the parameters used for the major absorption components, and the energies, intensities, and widths of these minor components cannot be unequivocally assigned. For all fits reported, the correlation coefficient was $r^2 \geq 0.995$.

D. Emission Spectroscopy. Ambient emission spectra were determined with a Spex Fluorolog spectrometer. All spectra were corrected using the Spex instrument correction factor. Spectral deconvolution was accomplished as described for absorption except for the scaling, which was accomplished by dividing the experimental emission intensity by ν_{em}.[60]

E. Electrochemistry. The electrochemical results were obtained with a Princeton Applied Research model 273 electrochemical system and a model 173 potentiostat/galvanostat equipped with a PAR model 179 digital coulometer and a model 175 universal programmer or with a BAS model 100A electrochemical workstation using manufacturer-supplied software for instrument control and data manipulation.

Cyclic voltammograms were obtained using a three-electrode system consisting of a Ag/AgCl reference electrode, a Pt wire counter electrode, and a Pt disk working electrode for measurements in CH_3CN. The working electrode was polished with 0.3 and 0.05 μm Buehler alumina suspensions on a Buehler polishing cloth and sonicated for a few seconds between polishing cycles. The solutions consisted of the complex dissolved in acetonitrile containing 0.1 M TEAP (tetraethylammonium perchlorate) or TBAH (tetrabutylammonium hexafluorophosphate) as electrolyte. Cyclic voltammograms were generally referenced internally to ferrocene (0.437 V vs Ag/AgCl) or to diacetylferrocene (0.925 V vs Ag/AgCl)[62] dissolved in the sample solutions in acetonitrile. Electrochemistry in aqueous solutions with 0.1 M $(NH_4)_2SO_4$ was performed with

(55) Chang, J. P.; Fung, E. Y.; Curtis, J. C. *Inorg. Chem.* **1986**, *25*, 4233.
(56) Salaymeth, F.; Berhause, S.; Yusof, R.; de la Rosa, R.; Fung, E. Y.; Matamoros, R.; Law, K. W.; Zhen, Q.; Kober, E. M.; Curtis, J. C. *Inorg. Chem.* **1993**, *32*, 3895.
(57) Dixon, N. E.; Lawrence, A.; Lay, P. A.; Sargeson, A. M.; Taube, H. *Inorg. Synth.* **1986**, *24*, 243.
(58) Supporting material, see paragraph at end of paper.
(59) Callahan, R. W.; Brown, G. M.; Meyer, T. J. *Inorg. Chem.* **1975**, *74*, 1443.
(60) Gould, I. R.; Noukakis, D.; Luis, G.-J.; Young, R. H.; Goodman, J. L.; Farid, S. *Chem. Phys.* **1993**, *176*, 439.
(61) Galactic Industries Corporation, Salem, NH.
(62) Song, X.; Lei, Y.; VanWallendal, S. V.; Perkovic, M.; Jackman, D. C.; Endicott, J. F.; Rillema, D. P. *J. Phys. Chem.* **1993**, *97*, 3225.

Table 1. MLCT Spectra of Monometallic Polypyridyl Complexes[a]

complex [{D}(A)]	λ_{max} (nm) ($\epsilon_{max}/10^3$, M^{-1} cm^{-1}) [$\Delta\nu_{1/2}/10^3$, cm^{-1}] band I	band II	other bands	solvent
$[\{(bpy)_2Ru\}(bpy)]^{2+}$	452 ± 1 (14.23)[b]			H_2O
	455 [1.9][e]			
	458 [1.9][e]			1:1 DMSO/H_2O
	451 ± 1[c]			CH_3CN
$[\{(bpy)(en)Ru\}(bpy)]^{2+}$	487 (11.2)[d]	345 (8.82)[d]		H_2O
	496[d]	348[d]		1:1 DMSO/H_2O
$[\{(bpy)(NH_3)_2Ru\}(bpy)]^{2+}$	490 (9.5)[d]	345 (7.65)[d]		H_2O
	490 [2.1][e]	355 [3.8][e]		1:1 DMSO/H_2O
	491[d]	348[d]		CH_3CN
$[\{(en)_2Ru\}(bpy)]^{2+}$	515 (3.96)[d]	365 (7.85)[d]		H_2O
	526[d]	370[d]		1:1 DMSO/H_2O
$[\{(NH_3)_4Ru\}(bpy)]^{2+}$	522 (4.4)[d]	366 (7.1)[d]		H_2O
	526 [2.2][e]	364 [4.2][e]		
	532	372		1:1 DMSO/H_2O
	524 (4.2)	364 (6.8)		CH_3CN
	521 [2.4][e]	364 [4.4][e]		
$[\{(bpy)_2Ru\}(dpp)]^{2+}$	478 (10)	426 (12)		H_2O
	481 (9) [2.0][e]	422 (12) [2.3][e]		
	470 (sh)[f]	430[f]		
	463 (sh, 11.5)[g]	439 (12)[g]		CH_3CN
$[\{(NH_3)_4Ru\}(dpp)]^{2+}$	546 (4.5)	456 ± 2 (4.8)	368 (5)[e]	H_2O
	543 [2.0][e]	422 [4.0][e]	329 [5.5]	
	541 (4.2)	458 (3.7)	366 (4.5)	CH_3CN
	547 [2.4][e]	434 [4.0][e]	364 [5.4][e]	
$[\{(bpy)_2Ru\}(dpq)]^{2+}$	530 (3.5)	423 (3.1)	351	H_2O
	517	426	360	CH_3CN
$[\{(NH_3)_4Ru\}(dpq)]^{2+}$	591 (2.8)	438 (1.3)	346 (8)	H_2O
$[\{(bpy)_2Ru\}(dpb)]^{2+}$	565 (3.1)	405 (4.6)	392 (4.8), 370	H_2O
	551	395	386, 370	CH_3CN
$[\{(NH_3)_4Ru\}(dpb)]^{2+}$	619 (4.9)	427 (3.1)	386 (11.3), 367 (11)	H_2O
	606	430	385, 369	CH_3CN

[a] 1 cm path; 298 K. Uncertainty in λ_{max} is about ±1 nm. Uncertainties in extinction coefficient and bandwidth are about ±10%. Band energies, intensities, and widths are based on absorption band envelopes except as indicated. [b] Average values are from the following. Lin, C. T.; Boettcher, M.; Chou, M.; Creutz, C.; Sutin, N. *J. Am. Chem. Soc.* **1976**, *98*, 212. Harriman, A. *J. Chem. Soc., Chem. Commun.* **1977**, *777*. McClanahan, S. F.; Dallinger, R. F.; Holler, F. J.; Kincaid, J. R. *J. Am. Chem. Soc.* **1985**, *107*, 4853. [c] Average values are from the following. Nakamura, K. *Bull. Chem. Soc. Jpn.* **1986**, *59*, 7872. Juris, A.; Balzani, V.; Belser, P.; von Zelwesky, A. *Helv. Chim. Acta* **1981**, *64*, 2175. Kawanishi, Y.; Kitamura, N.; Kim, Y.; Tazuke, S. *RIKEN Q.* **1984**, *78*, 212. [d] This work and ref 82. [e] Estimate based on Gaussian deconvolution. [f] Brewer, K. J.; Murphy, W. R., Jr.; Spurlin, S. R.; Petersen, J. D. *Inorg. Chem.* **1986**, *25*, 882. [g] Reference 8.

ITO (indium−tin oxide) or glassy carbon working electrodes and referenced to Ag/AgCl.

F. Infrared Spectroscopy. Infrared spectra were obtained as KBr pellets using a Nicolet 760SX FT-IR and a Nicolet 680 DSP workstation. Spectral grade KBr used for all pellets was obtained from Aldrich and used without further purification. The KBr and all samples were dried in a vacuum oven at 80−100 °C for several hours.

G. Molecular Orbital Calculations. Computations were carried out with the Gaussian series of electronic structure programs.[63] Geometries were fully optimized at the HF/LANL2DZ level of theory. This consists of the Los Alamos pseudopotentials on heavy atoms and the D95V all-electron basis on first- and second-period atoms. To simulate the change in conformation of the ligands on complexation, the dpp, dpq, and dpb ligand geometries were also optimized with one and two Zn^{2+} bound. An estimate of the trends in the MLCT excitation energies can be obtained from Koopman's theorem, i.e., from the orbital energies of the free ligands in the conformations indicated. Even though accurate excitation energies cannot be obtained from the orbital energies alone, changes in the energies of the unoccupied orbitals of the ligands should parallel trends in the MLCT excitation energies that are due to differences in the ligands. To obtain approximate values of the metal-independent variations of MLCT energies for systematic comparison to the calculated ligand orbital energies, we have subtracted the M^{III}/M^{II} half-wave potentials from the observed absorption band energies.

(63) Frisch, M. J.; Trucks, G. W.; Schlegel, H. B.; Scuseria, G. E.; Robb, M. A.; Cheeseman, J. R.; Zakrzewski, V. G.; Montgomery, J. A., Jr.; Stratmann, R. E.; Burant, J. C.; Dapprich, S.; Millam, J. M.; Daniels, A. D.; Kudin, K. N.; Strain, M. C.; Farkas, O.; Tomasi, J.; Barone, V.; Cossi, M.; Cammi, R.; Mennucci, B.; Pomelli, C.; Adamo, C.; Clifford, S.; Ochterski, J.; Petersson, G. A.; Ayala, P. Y.; Cui, Q.; Morokuma, K.; Malick, D. K.; Rabuck, A. D.; Raghavachari, K.; Foresman, J. B.; Cioslowski, J.; Ortiz, J. V.; Stefanov, B. B.; Liu, G.; Liashenko, A.; Piskorz, P.; Komaromi, I.; Gomperts, R.; Martin, R. L.; Fox, D. J.; Keith, T.; Al-Laham, M. A.; Peng, C. Y.; Nanayakkara, A.; Gonzalez, C.; Challacombe, M.; Gill, P. M. W.; Johnson, B. G.; Chen, W.; Wong, M. W.; Andres, J. L.; Head-Gordon, M.; Replogle, E. S.; Pople, J. A. *Gaussian 98*; Gaussian, Inc.: Pittsburgh, PA, 1998.

Results

Information on the MLCT spectroscopy and electrochemistry of several types of simpler D/A systems provides bases for the comparison and interpretation of the relatively complex MLCT properties of the dipyridylpyrazine class of complexes; Table 1 summarizes the MLCT spectra of several types of polypyridyl-containing ruthenium(II) complexes, and Table 2 summarizes the MLCT spectra of bimetallic complexes. Table 3 summarizes the electrochemical behavior of these complexes, and Table 4 summarizes the results of the numerical calculations on the polypyridyl ligands.

The scaled absorbance of $[Ru(NH_3)_4bpy]^{2+}$ shows two MLCT bands that do not have a Gaussian band shape (Figure 2). Since the deviations from Gaussian shape correspond to

Table 2. MLCT Spectra of Bimetallic Complexes[a]

complex [{D, D′}(A)]	λ_{max}(nm) (ϵ_{max}, M^{-1} $cm^{-1}/10^3$) [$\Delta\nu_{1/2}$,$cm^{-1}/10^3$] band I	band II	other bands	solvent
$[\{(bpy)_2Ru,Ru(bpy)_2\}(dpp)]^{4+}$	520 (21)	417 ± 2 (17)	330 (26)	H_2O
	512 (19) [2.8][b]	413 (16) [3.6][b]		
	524 ± 2[c] (20)	423 ± 2[c] (14)	330[c] (32)	CH_3CN
$[\{(NH_3)_4Ru,Ru(bpy)_2\}(dpp)]^{4+}$	539 ± 2 (6)	431 ± 2 (3.5)		H_2O
	536 (7)	429 (5)		CH_3CN
$[\{(NH_3)_4Ru,Ru(NH_3)_4\}(dpp)]^{4+}$ [d]	558 (19)	368 (9.8)	318 (25)	H_2O
$[\{(bpy)_2Ru,Ru(bpy)_2\}(dpq)]^{4+}$	614 (9.8)	608 (18.2)	530, 426	H_2O
$[\{(NH_3)_4Ru,Ru(bpy)_2\}(dpq)]^{4+}$	640 (4)	531 (9)	424 (8), 393 (10), 350 (17)	H_2O
	640 (3.5)	523 (7)	427 (6.5), 393 (8)	CH_3CN
$[\{(NH_3)_4Ru,Ru(NH_3)_4\}(dpq)]^{4+}$	700 (4) [5]	598 (5)	344 (13)	H_2O
	680 (5)	578 (5)	339 (12)	CH_3CN
$[\{(bpy)_2Ru,Ru(bpy)\}(dpb)]^{4+}$ [c]	646	410	368	H_2O

[a] 1 cm path; 298 K. Uncertainty in λ_{max} is about ±1 nm except as noted. Uncertainties in extinction coefficient and bandwidth are about ±10%. Estimates are based on band envelopes except as indicated. [b] Estimate based on Gaussian deconvolution (this work). [c] Average for this work and refs 8 and 12. [d] This work and ref 7.

Table 3. Half-Wave Potentials of the Complexes

complex [{D}(A)]	$E_{1/2}$, V $Ru(bpy)_2^{3+/2+}$	$Ru(NH_3)_4^{3+/2+}$	$L^{0,1-}$	$F\Delta E_{1/2}$, $cm^{-1}/10^3$	solvent
$[\{(bpy)_2Ru\}(bpy)]^{2+}$	1.26 ± 0.01[b]		−1.28 ± 0.03[b]	20.5 ± 0.2	H_2O
	1.27 ± 0.03		−1.34 ± 0.04	21.1 ± 0.5	CH_3CN
$[[(bpy)(en)Ru\}(bpy)]^{2+}$	0.88[c]		−1.51[c]	19.2	CH_3CN
$[\{(bpy)(NH_3)_2Ru\}(bpy)]^{2+}$	0.82[c]		−1.51[c]	18.8	CH_3CN
$[\{(en)_2Ru\}(bpy)]^{2+}$	0.51[c]		−1.73[c]	18.1	CH_3CN
$[\{(NH_3)_4Ru\}(bpy)]^{2+}$	0.31[c,d]		−1.42[c,d]	14.1	H_2O
	0.50[c,d]		−1.70[c,d]	17.7	CH_3CN
$[\{(bpy)_2Ru\}(dpp)]^{2+}$	1.39 ± 2[d,e]		−1.01 ± 1[d,e]	19.4	CH_3CN
$[\{(NH_3)_4Ru\}(dpp)]^{2+}$		0.56[d]	−1.28[d]	14.8	H_2O
		0.76[d]	−1.30[d]	16.6	CH_3CN
$[\{(bpy)_2Ru\}(dpq)]^{2+}$	1.28[d]		−0.65[d]	15.6	H_2O
	1.43[d]		−0.82[d]	16.5	CH_3CN
$[\{(NH_3)_4Ru\}(dpq)]^{2+}$		0.88[d]			CH_3CN
$[\{(bpy)_2Ru\}(dpb)]^{2+}$	1.28[d]		−0.65[d]	15.6	H_2O
	1.45[d]		−0.82[d]	18.3	CH_3CN
$[\{(bpy)_2Ru,Ru(bpy)_2\}(dpp)]^{4+}$	1.56, 1.38 (±0.05)[d−f]		−0.64 ± 0.04[d−f]	17.7	CH_3CN
$[\{(NH_3)_4Ru,Ru(bpy)_2\}(dpp)]^{4+}$	1.32[d]	0.76[d]	−0.80[d]	12.6	CH_3CN
$[\{(NH_3)_4Ru,Ru(NH_3)_4\}(dpp)]^{4+}$		0.96, 0.57[d]	(−0.96)[g]	(12.3)[g]	CH_3CN
$[\{(NH_3)_4Ru,Ru(NH_3)_4\}(dpq)]^{4+}$		1.38, 0.89[d]			CH_3CN
$[\{(NH_3)_4Ru,Ru(bpy)_2\}(dpq)]^{4+}$	1.44[d]	1.02[d]			CH_3CN

[a] Sweep rate, 100−200 mV/s; electrolyte, 0.1 M TBAE or TBAH; Ag/AgCl reference electrode; ambient conditions. [b] Average of values is listed in the following. Juris, A.; Barigelletti, F.; Campangna, S.; Balzani, V.; Belser, P.; von Zelwesky, A. *Coord. Chem. Rev.* **1988**, *84*, 85. [c] Reference 82. [d] This work. [e] Average value is from the following. Brewer, K. J.; Murphy, W. R., Jr.; Spurlin, S. R.; Petersen, J. D. *Inorg. Chem.* **1986**, *25*, 882. Denti, G.; Campagna, S.; Sabatino, L.; Seroni, S.; Ciano, M.; Balzani, V. *Inorg. Chem.* **1990**, *29*, 4750. [f] Reference 8. [g] Extrapolated value based on related complexes.

Table 4. Comparison of Computed Orbital Energies (LUMO and LUMO + 1) and MLCT Energy Maxima (Bands 1 and 2) of $[(NH_3)_4Ru(L)]^{2+}$ [a]

ligand (L)	orbital	parent ring	free ligand	constrained with one metal	constrained with two metals	$h\nu_{max}$[b]
bpy	LUMO		15.39	15.5		19.16
bpy	LUMO + 1		21.62	21.7		22.12
dpp	LUMO	17.6 (α)	17.9 (α)	12.1 (β)	10.3 (β)	18.48
dpp	LUMO + 1	22.0 (β)	19.1 (β)	16.7 (α)	16.0 (α)	21.83
dpq	LUMO	11.6 (α)	11.9 (α)	10.5 (α)	9.8 (α)	16.9
dpq	LUMO + 1	21.1 (β)	16.5 (β)	13.4 (β)	11.5 (β)	22.8
dpb	LUMO	7.2 (α)	7.8 (α)	6.2 (α)	5.3 (α)	16.5
dpb	LUMO + 1	20.3 (β)	16.8 (β)	14.0 (β)	11.9 (β)	17.3

[a] All energies are in units of $cm^{-1}/10^3$. Computations were performed at the HF/LANL2DZ level of theory. [b] From absorption envelope in acetonitrile.

additional intensity contributions on the high-energy side of band 1 and the low-energy side of band 2, compensation for them requires a minimum of two relatively minor Gaussian components, as shown in the Gaussian fits at the top and middle of Figure 2. The transition energies, bandwidths, and intensities of the major and minor components were essentially the same in water and in acetonitrile. These minor fitting components a and b cannot be purely vibronic; the energy differences and intensities required are too large for a simple vibronic progression. Resonance Raman data for this complex[64] can be used to construct an absorption profile for the lowest energy MLCT band including the apparent vibronic contributions, shown at the bottom of Figure 2, and this profile requires additional electronic components (such as component a) in order to match the observed spectrum. The report of Streiff et al.[65] that components of band 1 are resolved in a 77 K methanol/ethanol glass is further support for this analysis. We tentatively assign the most intense component to the $d\pi_m$ orbital that has the largest overlap with the bpy LUMO. The

(64) Hupp, J. T.; Williams, R. T. *Acc. Chem. Res.* **2001**, *34*, 808.
(65) Streiff, J. H.; Edwards, W. D.; McHale, J. L. *Chem. Phys. Lett.* **1999**, *312*, 369.

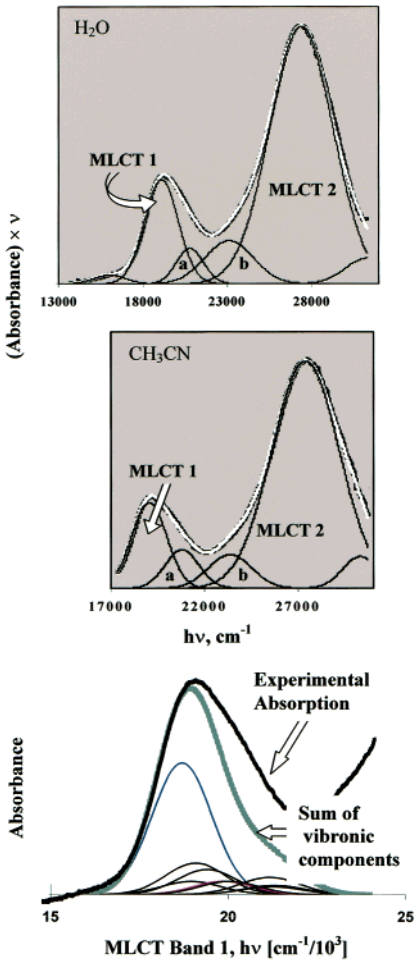

Figure 2. Scaled absorption spectra of $[Ru(NH_3)_4bpy]^{2+}$ in water and acetonitrile [(absorbance)(ν_{abs}) vs $h\nu_{abs}$]: experimental absorption envelope, heavy black line; sum of Gaussian fitting components, superimposed solid white line. For the Gaussian components (energies in cm^{-1}), $h\nu_{max}$ [$\Delta\nu_{1/2}$] in H_2O are the following: MLCT 1, 19 100 [2400]; MLCT 2, 27 400 [4400]; a, 20 800 [1870]; b, 23 100 [3400]. In CH_3CN, the values are the following: MLCT 1, 19 200 [2200]; MLCT 2, 27 400 [4200]; a, 20 800 [2100]; b, 23 400 [2700]. The spectrum at the bottom of the figure compares the MLCT 1 absorption band in water (from the top spectrum) to the spectrum constructed from vibronic components, based on resonance Raman data reported in ref 64. We have assumed that all these vibronic components have a 2000 cm^{-1} bandwidth.

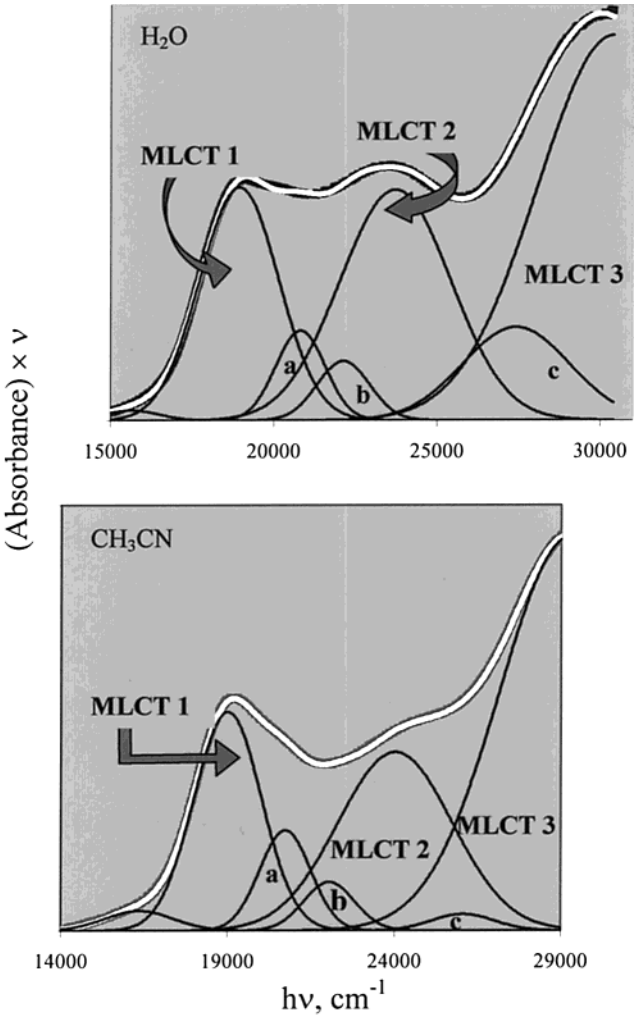

Figure 3. Scaled absorption spectra of $[Ru(NH_3)_4(dpp)]^{2+}$ (as in Figure 2). For the Gaussian components (energies in cm^{-1}), $h\nu_{max}$ [$\Delta\nu_{1/2}$] values in H_2O are the following: MLCT 1, 19 100 [2000]; MLCT 2, 23 716 [4000]; MLCT 3, 30 403 [5500]; a, 20 800 [1800]; b, 22 200 [1800]; c, 27 416 [3818]. In CH_3CN, the values are the following: MLCT 1, 19 010 [2384]; MLCT 2, 24 000 [4040]; MLCT 3, 29 100 [5430]; a, 20 700 [1800]; b, 22 000 [1800]; c, 26 000 [2200].

ab initio calculations indicate that the LUMO and LUMO + 1 of coordinated bpy both have b_1 (C_{2v}) symmetry.[50,66−70] Both π^* orbitals would mix with the $d\pi_m(b_1)$ orbital, and both transitions would be *z*-allowed.

We have resolved three distinct principle MLCT bands for $[Ru(NH_3)_4(dpp)]^{2+}$. The resulting absorption envelope was different in acetonitrile than in water (Figure 3). The Grams 32 based spectral deconvolution indicates that this difference is attributable to a smaller bandwidth of MLCT 1 in acetonitrile; the ratio of integrated band intensities (MLCT 1/MLCT 2) is nearly the same (0.73 in acetonitrile and 0.71 in water). The energies and integrated intensities of the principle MLCT bands do not appear to be significantly different in the two solvents. We have treated the component structure of this complex as similar to that of $[Ru(NH_3)_4(bpy)]^{2+}$ but with one additional, major MLCT band (Figure 3).

The three intense MLCT transitions observed for the $[Ru(NH_3)_4(dpp)]^{2+}$ complex in the visible−near-UV region, where only two are observed for $[Ru(NH_3)_4(bpy)]^{2+}$, suggest that there are more low-energy π^* acceptor orbitals in dpp than in bpy. If the energy differences were simply transferable, then the second Ru^{II}/dpp MLCT transition in $[Ru(bpy)_2(dpp)]^{2+}$ would occur at 24.6×10^3 cm^{-1}, very similar to the energy expected for the Ru^{II}/bpy transition. In acetonitrile the lowest energy MLCT absorption maxima of the monometallic complexes, $[Ru(NH_3)_5L]^{2+}$ and $[Ru(bpy)_2L]^{2+}$, correlate well with changes in the constituent half-wave potentials (Figure 4; slope = 0.9 ± 0.2, intercept = $(3 \pm 3) \times 10^3$ cm^{-1}, $r^2 = 0.9$; omitting the point for $[Ru(bpy)_2dpb]^{2+}$). The bimetallic complexes that contain $Ru^{II}(NH_3)_4$ deviate dramatically from this correlation.

The minimized structures calculated for the free ligands all have the pendant pyridines arranged with nitrogen atoms adjacent, and their rings are twisted by about 130° from the ideal orientation for coordination (see Figure 5). When the ligands are constrained to adopt a structure appropriate for

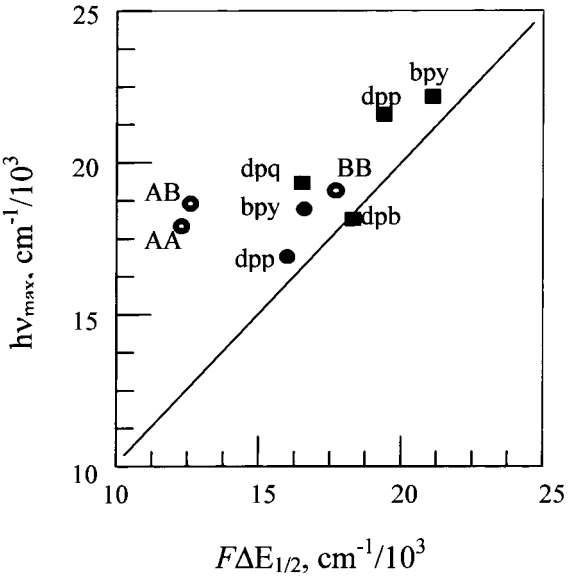

Figure 4. Correlation of band I absorption maxima with the difference in the half-wave potentials for Ru^{II} oxidation and ligand (L) reduction (*F* is Faraday's constant) in acetonitrile: solid squares for $[Ru(bpy)_2(L)]^{2+}$ complexes, solid circles for $[Ru(NH_3)_4(L)]^{2+}$ complexes (L as indicated on the figure); open circles for bimetallic complexes (BB, $[\{Ru(bpy)_2\}_2(dpp)]^{4+}$; AB, $[\{Ru(bpy)_2,Ru(NH_3)_4\}(dpp)]^{4+}$; AA, $[\{Ru(NH_3)_4\}_2(dpp)]^{4+}$). The ligand reduction potential used for AA was interpolated from the values observed for monometallic complexes $[\{Ru(bpy)_2\}_2(dpp)]^{4+}$ and $[\{Ru(bpy)_2,Ru(NH_3)_4\}(dpp)]^{4+}$. The solid line is drawn with a slope of 1.0 and a zero intercept.

bidentate coordination (modeled in the calculations by binding to Zn^{2+}), the pyridine rings are splayed and the pyrazine moiety is twisted (see Figure 1). The changes shown in Figure 5 are also representative of dpq and dpb. In the unconstrained geometries, the LUMO's of dpp, dpq, and dpb correlate with the LUMO's of pyrazine, quinoxaline, and benzoquinoxaline (Figures 6 and 7) and the nodal pattern is designated by α in Table 4. Likewise, the LUMO + 1's correlate and their nodal pattern is designated by β in the Table. As can be seen from Table 4, the conformations of the 2-pyridyl substituents have very little effect on the energy of the LUMO, but they can lower the LUMO + 1 energy significantly. In conformations suitable for bidentate coordination, the pyridyls are more nearly coplanar with the rest of the ring system and can interact more strongly. The

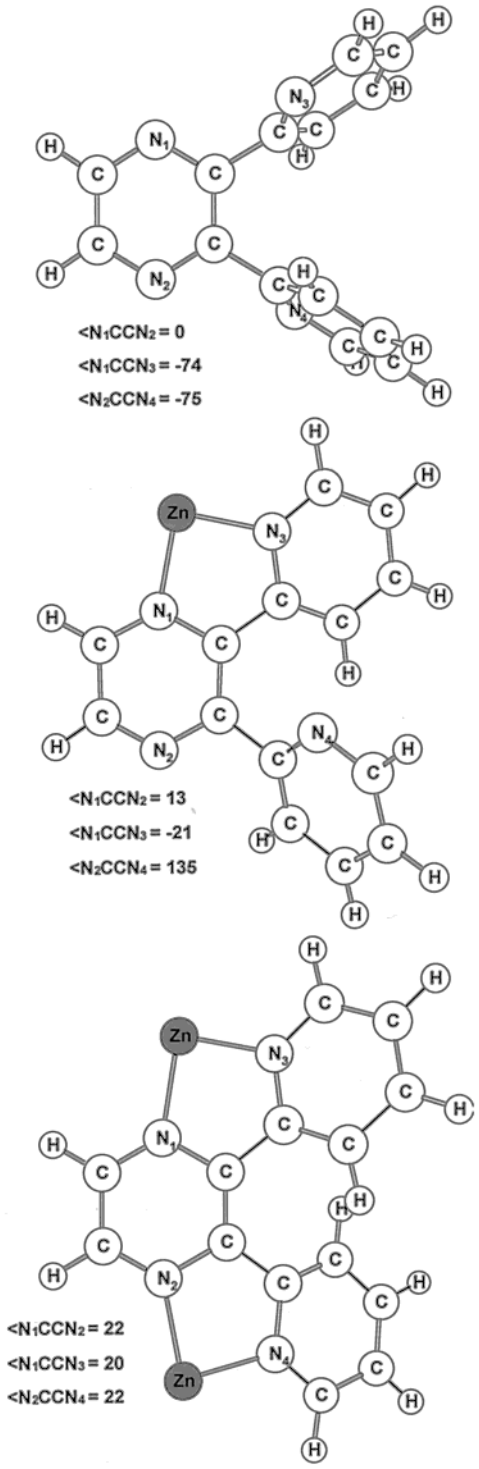

Figure 5. Minimized stereochemistries of dpp: top, free ligand; middle, constrained to coordinate one metal; bottom, constrained to bridge two metals. The Zn atoms have been highlighted in dark-gray.

(66) The details of this assignment will be discussed elsewhere. In brief, there are two principle issues: (a) the π^* orbital sequence corresponding to the observed dominant MLCT bands and (b) the assignment of the minor electronic components. In regard to issue a: (1) the lowest energy π^* orbitals of pyridine do not differ greatly in energy and correlate with the degenerate orbitals of the LUMO of benzene (we label the π^* orbital with a nodal plane passing through two atoms as β, the other as α); the ab initio calculations indicate that the two lowest energy π^* orbitals of planar bpy are of the form $(\alpha + \alpha)$ and $(\beta + \beta)$. This contrasts with the more common assignment of $(\alpha + \alpha)$ and $(\alpha - \alpha)$, respectively, based either on the simplifying neglect of the higher energy pyridine orbital[67,68] or on semiempirical MO calculations.[50,65] Other sequences have also been proposed.[70] In regard to issue b: In a simple orbital model of the complex, one of the $d\pi$ orbitals (labeled $d\pi_m$; note that the C_2 symmetry axis bisects the Cartesian angles of the metal complex, and symmetry adaption of the usual Cartesian $d\pi$ orbital set is required) mixes with the bpy LUMO, resulting in electron delocalization and a decrease in the energy of $d\pi_m$ (this is illustrated in Figure S4 of Supporting Information). The electron density delocalized from $d\pi_m$ to the bpy LUMO in the ground state could increase the electron−electron repulsions for transitions involving the other $d\pi$ orbitals, leading to an energy higher than expected on the basis of only orbital energy considerations. There are, of course, lower energy, very weak absorption contributions that probably are the convolution of hot band and triplet contributions, and there may be MLCT bands at energies outside the spectral window presented in Figure 2.

(67) Zwickel, A. M.; Creutz, C. *Inorg. Chem.* **1971**, *10*, 2395.
(68) Parker, W. L.; Crosby, G. A. *Int. J. Quantum Chem.* **1991**, *39*, 299.
(69) Ivanova, N. V.; Sizov, V. V.; Nikolskii, A. B.; Panin, A. I. *J. Struct. Chem.* **1999**, *40*, 620.
(70) Mulliken, R. S.; Person, W. B. *Molecular Complexes*; Wiley-Interscience: New York, 1967.

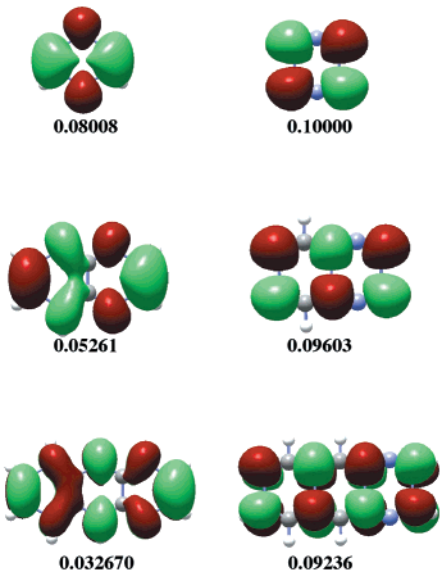

Figure 6. LUMO (left) and LUMO + 1 (right) for the parent rings of the bridging ligands, from top to bottom: dpp, dpq, and dpb. Orbital energies are listed in hartrees.

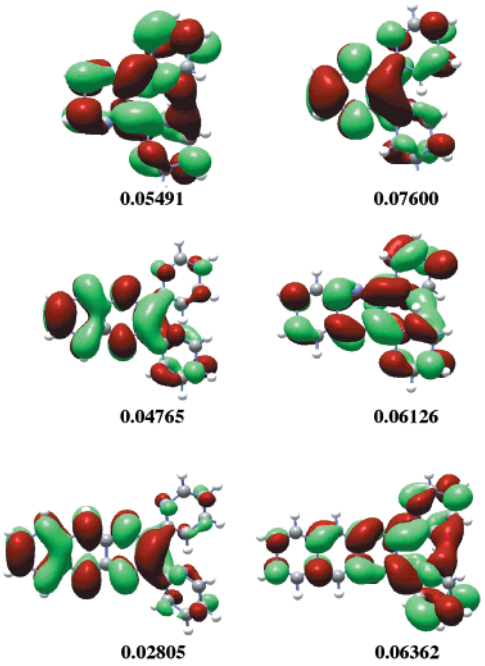

Figure 7. LUMO (left) and LUMO + 1 (right) of dpp, dpq, and dpb (top to bottom) constrained to a geometry appropriate for the bidentate coordination of one metal. Orbital energies are listed in hartrees.

interaction is greater for LUMO + 1, and its energy is lowered more. In dpp, the LUMO and LUMO + 1 are close in energy, and the effect of twisting one or both pyridyls into bidentate conformations is to push the energy of the original LUMO + 1 below that of the original LUMO, inverting their order. In dpq and dpb, the LUMO and LUMO + 1 separation (in the pyrazine moiety) is larger and the order is not inverted, despite the strong interaction between the pyridyls and the LUMO + 1's.

The calculated orbital energies of these ligands changed dramatically when Zn^{2+} was bound. This was most pronounced for the LUMO with the maximum orbital coefficients on the pyrazine nitrogens (e.g., the LUMO of pyrazine) and resulted in a change of the sequence of LUMOs in the dpp ligand. This is clearly an electrostatic effect of the vacuum calculation with a bare Zn^{2+} ion, and its relevance to the spectra of coordination complexes in the condensed phase is not clear. In contrast, the MLCT 1 energies correlate well with the LUMO energies calculated with the ligands configured for coordination but without the dipositive metal (Figure 8).

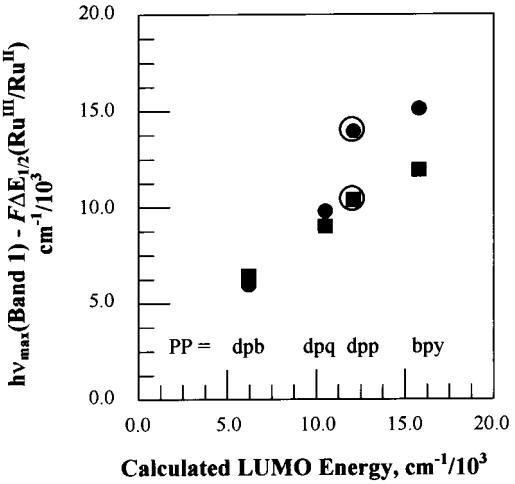

Figure 8. Comparison of the computed ligand LUMO energies with the lowest energy (in acetonitrile estimated from band envelopes) MLCT absorption maxima approximately corrected for variations in the metal contribution by subtracting $F\Delta E_{1/2}(Ru^{III}/Ru^{II})$. LUMO energies are computed for the ligand (without metal) configured for coordination of one metal: closed squares, $[Ru(bpy)_2(PP)]^{2+}$; closed circles, $[Ru(NH_3)_4(PP)]^{2+}$. The ligand LUMO is the α-type for all except dpp (circled points).

Emission band energies and N−H stretching frequencies are summarized in Table 5. The ambient ($DMSO/H_2O$) emission spectra of $[Ru(NH_3)_2(bpy)_2]^{2+}$ and $[Ru(bpy)_3]^{2+}$ were fit to three Gaussian components (Figure S5[58]). Emission bandwidths were smaller, and the vibronic structure was better resolved in glasses at 77 K than in ambient solutions, as illustrated for $[Ru(bpy)_2dpp]^{2+}$ in Figure 9.

The N−H stretching regions of the infrared for the PF_6^- salts of the ammine complexes were complicated by the O−H stretching frequencies of water. Extensive drying and careful handling of the samples reduced the O−H contribution. The N−H bands of the tetraammines were broad with little indication of structure and were very similar in energy; the band maxima (selected by the instrument program) varied over about a 40 cm^{-1} range depending on sample preparation. The $[Ru(NH_3)_2(bpy)_2]^{2+}$ complex exhibited two relatively sharp bands of very different intensity; both bands were significantly higher in frequency than the N−H stretches of the tetraammines (about 30 and 100 cm^{-1}).

Discussion

In the course of this study we have found a number of features of the dipyridylpyrazine class of ligands that have been a challenge to understand, even without the conceptual problems that are intrinsic to linked mixed-valence systems. The synthesis of complexes with a variety of second metals has been difficult, probably as a consequence of the

Table 5. Ambient Emission, N−H Stretching Frequencies, and Derived Parameters of Am(m)ine−Polypyridine−Ruthenium(II) Complexes

complex	$h\nu_{max}$(em)[a] [$\Delta\nu_{1/2}$]	ν_{NH}[b]	$\chi_{exch}^{M(0)}$ [c] ($^1/_2\chi_{reorg}^{D(0)}$)	$\Delta h\nu$[d]	f[e]	E_{DA}^{00} [f]	λ_r[g]	α_{DA}^2 [h]	E_{ST}[i]
$[Ru(NH_3)_6](Cl)_3$		3077[j]	13.6						
$[Ru(NH_3)_6](Cl)_2$		3315, 3210[j]	13.6						
$[Ru(NH_3)_6](PF_6)_3$		3185	13.6		1				
$[Ru(NH_3)_6](PF_6)_2$		3360 ± 20	13.6		0				
$[Ru(NH_3)_4bpy](PF_6)_2$		3250 ± 20	11.2		0.6 ± 0.2	16.9	2.1	0.09	
			(4.5)						
$[Ru(NH_3)_2(bpy)_2](PF_6)_2$	13.7 [1.8]	3357, 3258	9.1	6.5	0.2 ± 0.1[k]	(15.1)	3.8	0.08	3.2 ± 0.5
			(3.4)				(1.4)		
$[Ru(NH_3)_4dpp](PF_6)_2$		3250 ± 20	(4.5)		0.6 ± 0.2		1.8		
$[\{Ru(NH_3)_4\}dpp\{Ru(bpy)_2\}](PF_6)_4$		3241							
$[Ru(bpy)_3](Cl)_2$	16.2 [2.0]		6.8	5.6		(18.0)	3.9	0.07	1.3 ± 0.8
			(2.3)				(1.8)		
$[Ru(bpy)_2dpp](PF_6)_2$	14.5 [1.8]		~6.8	6.6			1.4		3 ± 1
							(1.4)		

[a] In DMSO/H_2O (1:1) at 300 K. Bandwidths from a Gaussian fit of the (corrected and scaled) emission using Grams 32. Energies in $cm^{-1}/10^3$. [b] In KBr pellet. ν_{NH} in units of cm^{-1}. [c] $\chi_{exch}^{M(0)}$ based on bimolecular self-exchange electron-transfer reactions (ref 38). $\chi_{exch}^{D(0)} = 2\chi_{exch}^{M(0)}/3$, with $\chi_{exch}^{M(0)}$ for the $[Ru(NH_3)_6]^{3+,2+}$ or the $[Ru(bpy)_3]^{3+,2+}$ couple and assuming that the polupyridyl ligand occupies $\sim^1/_3$ of the complex coordination sphere. Energies in $cm^{-1}/10^3$. [d] $\Delta h\nu = h\nu_{max}(abs) - h\nu_{max}(em)$. Energies in $cm^{-1}/10^3$. [e] $f = [\nu_{NH}(Ru^{II}(NH_3)_6) - \nu_{NH}(complex)]/[\nu_{NH}(Ru^{II}(NH_3)_6) - \nu_{NH}(Ru^{III}(NH_3)_6)]$. [f] $E_{DA}^{00} = h\nu_{max}(abs) - 2\lambda_{reorg}(a)$ ($E_{AD}^{00} = h\nu_{max}(em) + 2\lambda_{reorg}(e)$). Energies in $cm^{-1}/10^3$. [g] $\lambda_{reorg}(a)$ ($\lambda_{re9org}(e)$). Energies in $cm^{-1}/10^3$. [h] Based on eq 8. [i] Based on eq 19. Energies in $cm^{-1}/10^3$. [j] Deak, A.; Templeton, J. L. *Inorg. Chem.* **1980**, *19*, 1075. Griffith, W. P. *J. Chem. Soc. A* **1966**, 899. From a tabulation in ref 85. [k] Based on weighted average of ν_{NH}.

accompanying stereochemical distortions. Three visible−near-UV MLCT transitions of roughly comparable intensity are observed in $[(NH_3)_4Ru\text{-}dpp]^{2+}$, but only two are observed in this energy region for $[\{(NH_3)_4Ru\}_2dpp]^{4+}$, and the lowest energy transition is about 4 times as intense in the dimer as in the monomer. In a comparison of the lowest energy MLCT transitions with electrochemical data for these complexes, it appears that the metal and ligand additivity relations that are expected[31] in such systems do not hold. We have made 1:1 electrochemical/optical/theoretical comparisons of monometallic bpy and dpp complexes to facilitate evaluation of the properties of the dpp complexes. To address the issues raised by these observations, we have considered whether the spectroscopic and electrochemical peculiarities of the dpp complexes might arise from (a) unusual contributions of the reorganizational energy, (b) unusual features of the ligand electronic structure, and/or (c) properties that arise from donor−acceptor mixing (e.g., η_{DA} or Γ_{DA} in eqs 1 and 2). These contributions are most readily assessed with respect to a limit in which the D/A mixing is very small.

A. Spectroscopic, Kinetic, and Electrochemical Correlations in Simple D/A Systems. A.1. General Features and Expectations. Donor−acceptor complexes typically give rise to an optical absorption whose energy can be related to ionization energies and electron affinities[31,70,71] or to electrochemical potentials.[31,33] When there is strong electronic coupling between the donor and the acceptor, manifested by an intense charge-transfer absorption band, this can result in configurational mixing that perturbationally[70,72,73] alters the properties of both the donor and the acceptor. In a simple perturbation theory analysis,[70] the ground state is stabilized by an amount $\epsilon_s = [(H_{DA})^2/(1 + \alpha_{DA}^2)]/E_{DA}$, where $H_{DA} = \langle\psi_E^o|H|\psi_G^o\rangle$ is the electronic coupling matrix element, ψ_E^o and ψ_G^o are the unmixed excited and ground-state wave functions (in our treatment they represent the isolated donor and the isolated acceptor in the same medium[74]), and H is a Hamiltonian operator; the Franck−Condon (FC) excited state is destabilized by an equal amount.[70] This mixing alters the properties of the donor-metal and acceptor-ligand in the complex relative to those of the isolated donor and acceptor. The magnitude of this change in properties depends on both the donor and the acceptor and is not easily factored into individual contributions of the components. In the simplest perturbation theory limit, eqs 4a and 4b

$$\psi_G = \frac{\psi_D^{\,o} + \alpha_{DA}\psi_A^{\,o}}{(1 + \alpha_{DA}^{\,2})^{1/2}} \tag{4a}$$

$$\psi_E = \frac{\psi_A^{\,o} - \alpha_{AD}\psi_D^{\,o}}{(1 + \alpha_{AD}^{\,2})^{1/2}} \tag{4b}$$

where $\alpha_{DA} = H_{DA}E_{DA}$, molecular properties can be interpreted in terms of the fraction of charge delocalized, $\alpha_{DA}^2/(1 + \alpha_{DA}^2)^{1/2}$, between the donor and acceptor (for simplicity, we omit the normalization factors in the remaining discussion; all α_{IJ} and H_{IJ} parameters below are understood to be normalized). The mixing could alter either the Coulomb or the exchange integral terms.[31,46]

While it is clear that electron exchange contributions to the state energies are not insignificant, the changes in exchange energy that result from configurational mixing must be small. A lower limit, $\Delta K_g \leq 10\%$, can be based on the ratio of the excited-state exchange energy to the total transition energy ($\sim 2K_e$ out of about 20×10^3 cm^{-1}) and $\epsilon_s = \alpha_{DA}^2 E_{DA}$ (where α_{DA}^2 must be less than or equal to 0.5), assuming that there are no exchange contributions to H_{DA}. The arguments that follow are based mostly on the charge delocalization interpretation.

(71) Lever, A. B. P. *Inorganic Electronic Spectroscopy*; Elsevier: Amsterdam, 1984.
(72) Newton, M. D. *Adv. Chem. Phys.* **1999**, *106*, 303.
(73) Newton, M. D. *Chem. Rev.* **1991**, *91*, 767.

(74) For purposes of the correlation of experimental observations, we define the reference states represented by ψ_D^o and ψ_A^o as the equivalent donor and acceptor, respectively, in the limit that coupling goes to zero, but all other conditions are the same.

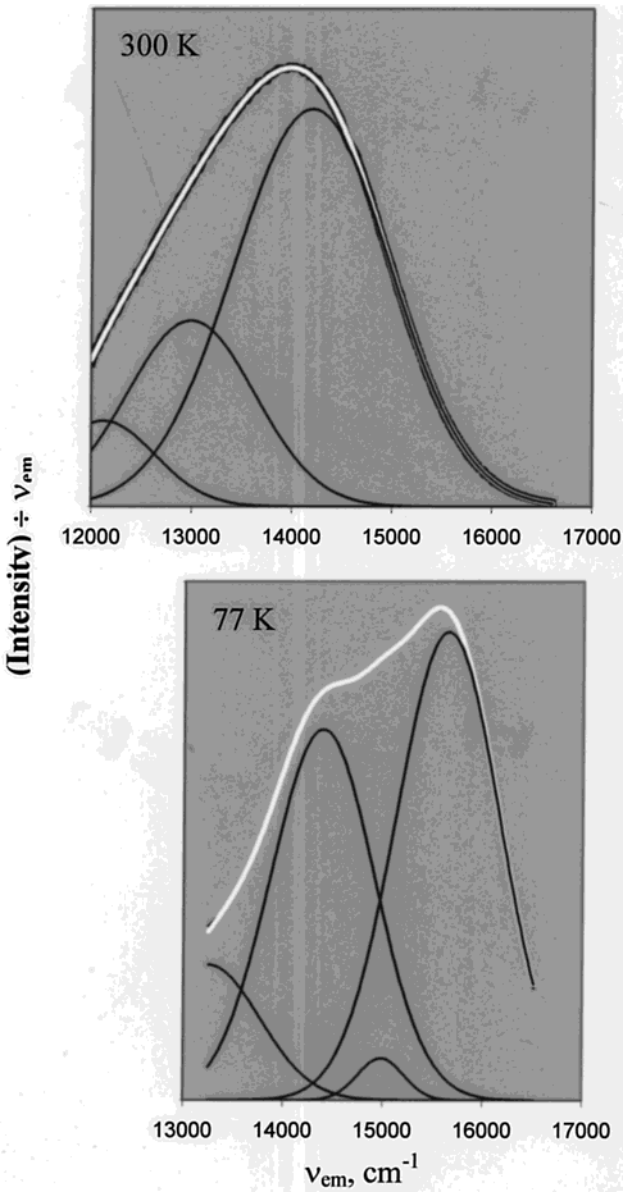

Figure 9. Emission of $[Ru(bpy)_2dpp]^{2+}$ in $DMSO/H_2O$; top, ambient solution; bottom, 77 K glass. For the Gaussian components in ambient solution (energies in cm^{-1}), $h\nu_{max}$ [$\Delta\nu_{1/2}$] values are the following: 14 200 [1843]; 13 000 [1505]; 12 100 [1219]. For the major Gaussian components in 77 K glass (energies in cm^{-1}), $h\nu_{max}$ [$\Delta\nu_{1/2}$] values are the following: 15 700 [1157]; 14 300 [1404]; 13 000 [1222]. The scaled experimental spectrum is a heavy dark line, and the fitted spectrum (sum of the Gaussian components) is the superimposed white line.

Variations in the charge distribution within a molecule are expected to result in variations in molecular bond lengths and angles, in solvation energy, and in certain vibrational frequencies. The correlated variations in the nuclear reorganizational and electrochemical parameters are used to characterize charge-transfer processes, and variations in these experimental parameters are often used to extract information about D/A mixing.[9,25,33,56,75] Values of reorganizational energies or vibrational frequencies are sensitive to the electronic charge distribution, while the singlet−triplet energy difference (E_{ST}) is mostly dependent on exchange terms ($E_{ST} \cong 2K_{exch}$; there should also be small contributions of nuclear and electronic relaxation).

A.2. Characterization of MLCT Excited States. The absorption of light to form the Franck−Condon excited state leaves the nuclei fixed, and this excited state will be vibrationally excited. In the limit that a single high-frequency mode ($h\nu_h > 4k_BT$) is excited and that there is a continuum of low-frequency modes ($h\nu_s < 4k_BT$ usually associated with the solvent), the absorptivity at a frequency ν_{abs} for the process in eq 5,

$$D-A + h\nu \rightarrow D^+-A^- \tag{5}$$

can be expressed as in eq 6,[60,76,77]

$$\epsilon(\nu_{abs}) = \frac{8N_A\pi^3}{3000h^2c\nu_{abs}\ln 10} n^3 H_{DA}{}^2(\Delta\mu_{DA})^2(FC) \tag{6}$$

$$FC = \sum_j F_j \exp\left[\frac{-(E_{DA}{}^{00} - h\nu_{abs} + jh\nu_h + \lambda_s)^2}{4\lambda_s k_B T}\right]$$

$$F_j = S^j \frac{\exp(-S)}{j!(4\pi\lambda_s k_B T)^{1/2}}$$

$$S = \frac{\lambda_h}{h\nu_h}$$

where $E_{DA}{}^{00}$ is the energy difference between the zeroth vibrational levels of the ground and excited state, λ_{vib} is the energy required to change the nuclear coordinates of the vibrationally equilibrated excited state (VEqES) into those of the ground-state PE minimum, and the reorganizational energy contributions corresponding to $h\nu_h$ and $h\nu_s$ to λ_{reorg} are λ_h and λ_s, respectively.[78] The energy of the absorption maximum is equal to the free energy change that occurs during the absorption of light. The dominant contributions to this process, based on the maximum of the FC function, are given by either eq 7a or eq 7b,

$$h\nu_{max} = E_{DA}{}^{00} + \lambda_{reorg} + ... \tag{7a}$$

$$h\nu_{max} = |\Delta G_{DA}{}^{00}| + \chi_{reorg} + ... \tag{7b}$$

provided the terms on the right-hand side of these equations are internally consistent: energy quantities for eq 7a and free energy quantities for eq 7b ($\chi_{reorg} = \chi_h + \chi_s$, analogous to the components of λ_{reorg}). $\Delta G_{DA}{}^{00}$ is the free energy difference between the vibrationally equilibrated ground and excited states, and χ_{reorg} is the free energy change associated with the change from the nuclear coordinates of the VEqES to those of the ground state. The experimental evaluations of free energy quantities are usually easier than of energy quantities, and most correlations of the components of optical

(75) de la Rosa, R.; Chang, P. J.; Salaymeth, F.; Curtis, J. C. *Inorg. Chem.* **1985**, *31*, 4229.
(76) Myers, A. B. *Acc. Chem. Res.* **1998**, *30*, 519.
(77) Graff, D.; Claude, J. P.; Meyer, T. J. In *Electron Transfer in Organometallic and Biochemistry*; Isied, S. S., Ed.; Advances in Chemistry Series 253; American Chemical Society: Washington, DC, 1997; Chapter 11, p 183.
(78) Note that the use of eq 6 assumes that H_{DA} and $\Delta\mu_{DA}$ are constant through the absorption band.

transition energies are in terms of electrode potentials determined for oxidation or reduction of the D/A system (eq 1).

A.3. Correlation with Electron-Transfer Parameters. A.3.a. Kinetic Parameters. The reorganizational parameters in eq 7b are often interpreted in terms of the component, electron-transfer activation free energies (from rate constant data).[39,41] This interpretation of the parameters is fundamentally based on the assumption that there is very little configurational mixing between donor and acceptor. Homogeneous solution electron-transfer kinetic data or ion pair charge-transfer spectra can be the bases for useful estimates of the reorganizational free energy, χ_{reorg}^{DA}, in the limit of little electronic mixing[32,38,40] (see Figure S6[58]). The reorganizational free energy is the sum of metal-fragment and ligand-fragment contributions and $\chi_{reorg}^{DA(0)} = {}^1/_2(\chi_M^{(0)} + \chi_L^{(0)})$. We have used aqueous self-exchange electron-transfer data to estimate values of χ_{reorg}^{DA} [38] and these values as the bases for estimating $\chi_M^{(0)}$ for several complexes (Table 5).[79]

A.3.b. Effect of Ground State−Excited State Mixing on Nuclear Reorganizational Energies. In the simple two-state limit (parabolic ground state and excited state PE surfaces with the same force constants), the excited state−ground state mixing results in a decrease in the separation of the PE minima by $(\alpha_{DA}^2 + \alpha_{AD}^2)x_0$, where x_0 is the separation in the absence of mixing (i.e., in the diabatic limit) and the subscripts correspond to coupling coefficients in the nuclear coordinates of the ground state and the excited state PE minima, respectively ($\alpha_{DA} = H_{DA}/E_{DA}$, $\alpha_{AD} = H_{DA}/E_{AD}$; $E_{AD} = E_{DA} - 2\lambda_{reorg}^0$). When D/A coupling is very strong, higher order terms may contribute to the attenuation of reorganizational energy ($\alpha_{AD} = z\alpha_{DA}$; see page S10[58]). Equation 8,

$$\lambda_{reorg}(a) \cong \lambda_{reorg}^0[1 - 4\alpha_{DA}^2 + \alpha_{DA}^4(1 + 2z^2 - z^4) + ...] \quad (8)$$

expresses higher order contributions to the reorganizational energy for the absorption process in the two-state limit.[80,81] The related expression for the emission from the same excited state is given in eq 9,

$$\lambda_{reorg}(f) \cong \lambda_{reorg}^0[1 - 2(1 + z^2)\alpha_{DA}^2 + \alpha_{DA}^4(1 + 2z^2 + z^4) + ...] \quad (9)$$

A.3.c. Electrochemical Parameters. When the experimental measure of ΔG_{DA}^{00} in donor−acceptor systems is based on the difference of half-wave potentials of the component couples,

$$D^+-A + e^- \rightleftarrows D-A, \quad E_{1/2}^{D} \quad (10a)$$

and

$$D-A + e^- \rightleftarrows D-A^-, \quad E_{1/2}^{A} \quad (10b)$$

then an additional term is required to relate eq 7b to eq 1.[31,33] The process in eq 5 is related to these couples by a one-electron-transfer equilibrium:[31,33]

$$D^+-A^- + D-A \rightleftarrows D^+-A + D-A^-, \quad K_{DA} \quad (11)$$

The combination of eqs 10 and 11 leads to eqs 5 and 12

$$-\Delta G_{DA}^{00} = F\Delta E_{1/2}^{D/A} - RT \ln K_{DA} \quad (12)$$

where $\Delta E_{1/2}^{D/A} = E_{1/2}^{A} - E_{1/2}^{D}$ and F is Faraday's constant. Substitution of eq 12 into eq 7b leads to

$$h\nu_{max} = -F\Delta E_{1/2}^{D/A} + RT \ln K_{DA} + \chi_{reorg}(a) + ... \quad (13)$$

Direct measurements of K_{DA} are not usually feasible for covalently linked D/A systems, but simple perturbation theory arguments lead to useful estimates. If the stabilization energy of the ground state that results from D/A mixing[70] is $\epsilon_s = H_{DA}^2/E_{DA}$, the destabilization of the VEqES is $\epsilon_d = H_{AD}^2/E_{AD}$. If K_{el} represents the strictly electrostatic contribution to K_{DA}, and ΔK_{exch} is the difference in exchange integral contributions (see page S8[58]), then eq 14 can be used:

$$RT \ln K_{DA} = -\epsilon_s + \epsilon_d + RT \ln K_{el} + \Delta K_{exch} \quad (14)$$

If we set $h\nu_{max} = E_{DA} = [E_{DA}^{00} + \lambda_{reorg}(a)]$, $E_{AD} = [E_{DA}^{00} - \lambda_{reorg}(a)]$, assume that $H_{DA} = H_{AD}$, and allow for the effect of the shift in the PE minima that results from D/A mixing ($\alpha_{DA}^2 x_0$ and $-\alpha_{AD}^2 x_0$, respectively) for the ground and excited states, then the ϵ_i are related as in eq 15 (see page S9[58]).[38,40]

$$\epsilon_d \cong \epsilon_s + 2\alpha_{DA}^2\lambda_{reorg}(a) + ... \quad (15)$$

Equation 13 may be rewritten as in eq 16,

$$h\nu_{max} \cong -F\Delta E_{1/2}^{D/A} + \chi_{reorg}(a)(1 + 2\alpha_{DA}^2) + RT \ln K_{el} + \Delta K_{exch} + ... \quad (16)$$

where we have assumed that free energy quantities may be substituted for energy quantities in the perturbational correction terms. The reorganizational parameter in eq 16 has the same meaning as that in eq 7b, and the correction terms arise only because $F\Delta E_{1/2}$ is not the same free energy quantity as ΔG_{DA}^{00} in eq 7b.

A.3.d. Electrostatic Contributions. The contributions of K_{el} may also be important. These can be factored into intermolecular and intramolecular contributions. The former amounts to an ion pair association constant and is expected to be small in high dielectric media. The intramolecular Coulombic term is the largest term for the D^+-A^- species in eq 11.

B. Strongly Coupled Systems and the Ru^{II}/bpy Paradigm. Arguments presented above indicate that charge

(79) Note that $\chi_{reorg}^{DA} = {}^1/_2(\chi_{reorg}^{D} + \chi_{reorg}^{A})$ and that each reorganizational energy contribution is the sum of contributions (χ_s^X and χ_h^X) from the low-frequency (largely solvent) and high-frequency (molecular) vibrational modes, respectively, that correlate with the solvational and structural differences of the ground and excited states.

(80) Equation 3, when applied to emission, implies similar mixing at both minima; this would only be the case for the two-state limit if the minima have the same PE or if λ_{reorg} is very small; see page S9 of Supporting Information and ref 81.

(81) Matyushov, D. V.; Newton, M. D. *J. Phys. Chem.* **2001**, *106*, 8516.

delocalization can attenuate both the low-frequency and the high-frequency vibrational contributions to the reorganizational free energy in strongly coupled systems. Conversely, the attenuation of these vibrational contributions to the reorganizational energy could be a measure of the amount of charge delocalized.

B.1. MLCT Spectra of $[Ru(NH_3)_4bpy]^{2+}$. The MLCT absorption spectra of this complex in water and acetonitrile are very similar, but the resolved Gaussian bandwidth of the dominant lowest energy component is about 10% larger in water. Equation 17,

$$\Delta\nu_{1/2} \cong \sigma + 4[k_B T\lambda_s \ln 2]^{1/2} \qquad (17)$$

(where σ is the standard deviation from the mean values of $E_{DA}{}^{00}$ and λ_{reorg}; see page S10[58]) with $\sigma = 0$ implies that $\lambda_s \approx 2.1 \times 10^3$ in water, significantly smaller than even the value of $^1/_2\chi_{reorg}{}^D$ in Table 5. Since $\lambda_s{}^0 = {}^1/_2(\lambda_s{}^D + \lambda_s{}^A)$ and assuming that $\lambda_s{}^D \cong \chi_{reorg}{}^D$ and $\lambda_s{}^A \approx 9000$ cm^{-1} (see below), with $\lambda_s \cong \lambda_{reorg}(a)$ in eq 8, an iterative fit implies about 9% delocalization of electron density in this complex.

There is also evidence for attenuation of the reorganizational energy in the emission spectra of $Ru(Am)_{(6-2n)}(bpy)_n{}^{2+}$ complexes[82,83] (Am = am(m)ine). The observed bandwidths imply that $\lambda_s(e) \cong 1.8$ and 1.4 cm^{-1}/10^3, respectively, smaller and in the opposite order of the estimated values of $\chi_{reorg}{}^D$ (Table 5). This ordering of $\lambda_s(e)$ is consistent with the greater value of $\alpha_{DA}{}^2$ expected for the ammine complex and the resulting greater attenuation of reorganizational parameters. The intensity contributions of the high-frequency modes are also attenuated; the intensity ratios of the first and second Gaussian components of the ambient (DMSO/H_2O) emissions of $[Ru(bpy)_3]^{2+}$ and $[Ru(NH_3)_2(bpy)_2]^{2+}$ ($S = 0.74$ and 0.57, respectively) imply that $\lambda_h(e)$ is about 1.1 and 0.86 cm^{-1}/10^3, respectively (for $h\nu_h \approx 1500$ cm^{-1}). However, these "resolved" spectral components are probably the result of the convolution of contributions of several different vibrational modes[64] and their detailed interpretation is not clear. This general pattern of decreased intensities of vibronic components with increased electron delocalization is consistent with intensity contributions inferred from resonance Raman data for $[Ru(NH_3)_4bpy]^{2+}$ [64] ($S \approx 0.3$ for the sum of components with frequencies in the range 1300−1600 cm^{-1}).

B.2. Concerning the Exchange Integral Contribution. In principle, the exchange integral can be estimated from the absorption−emission energy difference,

$$h\nu_{max}(abs) - h\nu_{max}(em) \cong \lambda_{reorg}(a) + \lambda_{reorg}(f) + E_{ST} = \lambda_{reorg}(a) + \lambda_{reorg}(f) + 2K_{exch} \qquad (18)$$

(E_{ST} is the singlet−triplet energy difference) provided the reorganizational energies are known. The deconvoluted absorption and emission maxima are summarized in Tables 1 and 5, and when combined with the values of $\lambda_{reorg}(a) \cong 1900$ cm^{-1} and $\lambda_{reorg}(e) \cong 1400$ cm^{-1} from the observed (deconvoluted) bandwidths and eq 18, indicate that $2K_{exch} \approx (3.3 \pm 0.7) \times 10^3$ cm^{-1} for $[Ru(NH_3)_2(bpy)_2]^{2+}$ (for an uncertainty of about 10% in each bandwidth).[84] However, these values of λ_{reorg} are not consistent with eqs 8 and 9; these equations, combined with $\lambda_{reorg}(f)$, imply that the absorption bandwidth should have been about 25% larger than observed and $2K_{exch} \approx 2300$ cm^{-1}. This is even more of a problem for $[Ru(bpy)_3]^{2+}$: $\Delta\nu_{1/2}(abs) \leq \Delta\nu_{1/2}(em)$, contrary to expectation based on eqs 8, 9, and 17 ($\Delta\nu_{1/2}(abs) \cong 1.5\ \Delta\nu_{1/2}(em)$). This behavior is probably a consequence of more extensive inter-ring configurational mixing (and charge delocalization) in the Franck−Condon excited state (see section B.4) than in the emitting state. For $[Ru(bpy)_2]^{2+}$, $2K_{exch} \approx 2000$ cm^{-1} based on the observed bandwidth (probably an upper limit), and $2K_{exch} \approx 500$ cm^{-1} based on the emission bandwidth and eqs 8, 9, and 17. These estimates are comparable to the values that Lever and Gorelsky[46] calculated, $2K_{exch} = 1460$ cm^{-1} for $[Ru(bpy)_3]^{2+}$ and (interpolated from calculated values) 2800 cm^{-1} for $[Ru(NH_3)_2(bpy)_2]^{2+}$; the ordering of the experimental estimates of K_{exch} is consistent with the calculations.

B.3. N−H Stretch as an Indicator of Charge Delocalization. It is well-known that N−H stretching frequencies are very sensitive to the charge on a metal center.[85] Unfortunately, they are also sensitive to the counterion and to other environmental factors.[85] However, the difference in ν_{NH} for $[Ru(NH_3)_6]^{2+}$ and $[Ru(NH_3)_6]^{3+}$ is sufficiently large, about 175 cm^{-1},[85] such that shifts in this frequency can be used as an indicator of the effective charge density on the metal. For this purpose, we define a fractional shift, f, for a complex:

$$f = \frac{\nu_{NH}(Ru^{II}(NH_3)_6) - \nu_{NH}(complex)}{\nu_{NH}(Ru^{II}(NH_3)_6) - \nu_{NH}(Ru^{III}(NH_3)_6)} \qquad (19)$$

These parameters are quite large for all the polypyridylammine complexes in this study (Table 5). In the simplest interpretation f is proportional to the amount of charge delocalized from Ru^{II} to the polypyridine ligand. Certainly the order of values of f, increasing with $[h\nu_{max}(MLCT\ 1)]^{-2}$, is consistent with this interpretation (Figure S12[58]). Appreciable charge delocalization is implied by the observed shifts in N−H stretching frequencies.

B.4. Electrochemical Observations on Polpyridine Complexes. We have inferred that eq 16 is appropriate for correlations involving the lowest energy MLCT transition. However, the *first* bipyridine ligand reduction of a series of $[L_{6-2n}Ru^{II}(bpy)_n]$ complexes (L an am(m)ine) occurs at increasingly negative potentials as n decreases (Table 3). This suggests significant electronic coupling between the bipyridine rings. Equation 20

$$\begin{bmatrix} -\epsilon & H_{BB} & H_{BB} \\ H_{BB} & \lambda_r - \epsilon & 0 \\ H_{BB} & 0 & \lambda_r - \epsilon \end{bmatrix} = 0 \qquad (20)$$

can be used to take account of ligand−ligand coupling (the vertical energy for moving the electron from one ring to another is the electron-transfer reorganizational energy, λ_r).

(82) Lei, Y. Ph.D. Dissertation, Wayne State University, Detroit, MI, 1989.
(83) Endicott, J. F.; Uddin, J. M. Work in progress.

There are three nondegenerate solutions of the secular equation. This is qualitatively consistent with observation. If the first reduction of $[(NH_3)_4Ru(bpy)]^{2+}$ is at $E_{1/2}^{o}$, then this argument suggests that the first reduction of $[Ru(bpy)_3]^{2+}$ will occur at $(E_{1/2}^{o} - 2(H_{BB})^2/\lambda_r)$ in the limit that $\lambda_r > H_{BB}$ (the general solution is $\epsilon_1 = [\lambda_r/2 - {}^1/_2(\lambda_r^2 + 8H_{BB}^2)^{1/2}]$). The related treatment of $[(NH_3)_2Ru(bpy)_2]^{2+}$ predicts that the first ligand reduction will occur at $(E_{1/2}^{o} - (H_{BB})^2/\lambda_r)$; see also Dodsworth et al.[86] The predicted trend in reduction potentials is qualitatively in accord with the observations. After taking account of the stabilization arising from Ru^{II}/bpy mixing and of the statistical effect contributed by the different numbers of polypyridyl rings in these complexes (for $[Ru(bpy)_3]^{2+}$ compared to $[Ru(NH_3)_4(bpy)]^{2+}$) and assuming that λ_r and H_{BB} are the same in each complex and that no other factors contribute, then the electrochemical observations indicate that each bipyridine−bipyridine interaction confers about $\epsilon_s(BB) \approx -0.1$ eV. This can be a basis for estimating λ_{reorg}^{L}. If we note that a $[(bpy)Ru^{II}(LL)(bpy^-)]^+$ complex is a mixed-valence complex in which the donor (bpy^-) and acceptor (bpy) are bridged by Ru^{II}, then standard superexchange arguments[72,73,87] predict that $H_{BB} \cong H_{ML}^2/(E_{ML})_{ave}$, for $H_{ML} \cong (7 \pm 1) \times 10^3$ cm^{-1} (eq 8; assuming that H_{ML} is independent of the distortion in the bpy^- ring; $(E_{ML})_{ave} = 2E_{ML}(E_{ML} - \lambda_{reorg}(a))/(2E_{ML} - \lambda_{reorg}(a))$ and $E_{ML} \cong 19 \times 10^3$ cm^{-1}, $H_{BB} \cong 2.7 \times 10^3$ cm^{-1} (this value of H_{BB} is somewhat larger than the values 1020 and 1660 cm^{-1} calculated by Lever and Gorelsky,[46] but their calculations are for the vertical MLCT excited state, which has (formally) a, Ru^{III} center and for which superexchange coupling may be smaller). Then $\lambda_r \approx 9 \times 10^3$ cm^{-1}. Since $H_{BB} \geq \lambda_r/4$, there may be little barrier to bpy/bpy^- electron transfer in the reduced ruthenium(II) complexes.

C. Application to the dpp Complexes. The dpp and bpy ligands of monometallic complexes exhibit very similar properties in each of the comparisons that we have made of monometallic complexes in this study. Many points made in the preceding section apply with only minor differences to the complexes containing the dpp ligand.

C.1. Features of MLCT Absorption Spectra. Several puzzling features of the spectra and electrochemistry noted above involve the comparison of monometallic and bimetallic complexes. Explanations for most of these observations can be based on the hypotheses that (a) the lowest energy MLCT band in the monometallic complexes involves the β-LUMO, (b) band II of the monometallic complexes involves the α-LUMO, and (c) the α-LUMO mediates very strong electronic coupling between Ru(II) and Ru(III) centers in the excited state, giving rise to a very large Jahn−Teller splitting of band II in bimetallic complexes. To accommodate the observations, the postulated explanations require that the β-LUMO contributes little to the Ru^{II}/Ru^{III} coupling.

C.2. Relevant Features of the ab Initio Calculations. It appears that orbitals of α and β types are similar in energy in most polypyridyl complexes and that both orbital types contribute to the low-energy MLCT transitions. The energies calculated for the LUMOs of bpy, dpp, dpq, and dpb correlate with the observed band I energies of the monometallic complexes (Figure 8; slopes of 1.0 ± 0.2 and 0.6 ± 0.1, respectively, for the ammine and bipyridine complexes when $F\Delta E_{1/2}$ is subtracted from $h\nu_{max}$ to approximately compensate for the variations of donor energy; this "correction" omits some contributions that result from metal−ligand mixing). The LUMO computed for the dpp ligand has β symmetry, while the LUMOs of dpq and dpb have α symmetry. The strong correlation of the calculated LUMO and the observed band 1 MLCT transition energies (Figure 8) is support for this inversion of the order of LUMOs in dpp. Note that this approach to the assignment is consistent with the arguments used throughout this paper that the properties of the complexes can be described as the sum of (1) the properties of the isolated metal, (2) the properties of the isolated ligand, and (3) perturbation theory based correction terms.

The rotation of one pyridine from a position nearly orthogonal to the pyrazine ring (dihedral angles of 75°) to a position appropriate for bidentate coordination of a metal (dihedral angle of 21°) results in a calculated decrease in the energy of the β-LUMO of about 7×10^3 cm^{-1}, while the energy of the α-LUMO changes by only about 1×10^3 cm^{-1}. This can be interpreted as a stabilization energy of $\epsilon_s(PP) \cong 7 \times 10^3$ cm^{-1} resulting from py−pz configurational mixing with the β-LUMO of pz and very little mixing with the α-LUMO. However, neither the α-LUMO nor β-LUMO changes much in energy when the second pyridine rotates into position for coordination of a second metal. This suggests that the stereochemical repulsion energy, which results in twisting of the pz ring, is approximately equal to $-\epsilon_s(PP)$. The net result is little change in LUMO energy, and this correlates with the observation that there is little difference in $h\nu_{max}$ for band I of the monometallic and bimetallic ammine complexes. The 1.8×10^3 cm^{-1} lower energy of band I in $[\{(bpy)_2Ru\}_2(dpp)]^{4+}$ than in $[(bpy)_2Ru(dpp)]^{2+}$ is attributable in part to the 1×10^3 cm^{-1} lower energy expected to result from bpy/dpp configurational mixing when the second metal $Ru(bpy)_2^{2+}$ moiety is coordinated to dpp (see Discussion, section B.4).

C.3. Electron Delocalization and Electron Exchange Contributions. We can make qualitative inferences and semiquantitative estimates of the significance of electron delocalization in the ground states of some of the dpp complexes. The N−H stretching frequencies imply that very similar amounts of electron density are delocalized in comparable bpy and dpp complexes. The emission spectra imply that λ_s is about 400 cm^{-1} smaller for $[Ru(bpy)_2dpp]^{2+}$ than for $[Ru(bpy)_3]^{2+}$; this suggests somewhat larger values of H_{DA} or smaller values of λ_{reorg}^{o} for the dpp complex. The differences in the energies of the lowest energy deconvoluted emission components differ only slightly from the respective

(84) Since E_{ST} is roughly comparable to the spin−orbit coupling energy for these complexes, we have assumed that $\lambda_{reorg}(f) \cong \lambda_s(e)$ in these estimates.

(85) Nakamoto, K. *Infrared and Raman Spectra of Inorganic and Coordination Compounds*; Wiley: New York, 1997; Part B.
(86) Dodsworth, E. S.; Vlcek, A. A.; Lever, A. B. P. *Inorg. Chem.* **1994**, *33*, 1045.
(87) Creutz, C.; Newton, M. D.; Sutin, N. *J. Photochem. Photobiol. A* **1994**, *82*, 47.

differences in metal and ligand half-wave potentials (the difference is larger for the dpp complex). These observations and the stronger attenuation of λ_s (eqs 3 and 8) suggest that both α_{DA} and $\lambda_{reorg}{}^{o}$ are somewhat larger in the dpp complex. Arguments presented above and observations summarized in Tables 1 and 5 indicate that $E_{ST} \cong (h\nu_{max}{}^{abs} - h\nu_{max}{}^{em} - \lambda_{reorg}{}^{abs} - \lambda_{reorg}{}^{em}) \cong 2K_{exch} \cong (3.4 \pm 1.0) \times 10^3$ cm^{-1} for the MLCT excited state of $[Ru(bpy)_2dpp]^{2+}$. This contrasts with an estimate of $2K_{exch} \approx (1.3 \pm 0.8) \times 10^3$ cm^{-1} for $[Ru(bpy)_3]^{2+}$ (Table 5).

C.4. Spectroscopic Splittings That Result from Ru^{II}/Ru^{III} Electronic Coupling. We have observed the Ru^{II}/Ru^{III} MMCT transition at 6.4×10^3 cm^{-1} in the $[\{(NH_3)_4Ru\}_2(dpp)]^{5+}$ complex.[23,88] This is comparable to the excited-state splitting (Jahn−Teller) of about 9.2×10^3 cm^{-1} proposed here for the vertical transition. It is not possible to examine this issue in the complexes containing $Ru(bpy)_2{}^{2+}$ because the Ru^{II}/bpy MLCT transition is expected at about the energy predicted for band II.

This suggests that the π^* orbitals of α symmetry are much more effective at mediating Ru^{II}/Ru^{III} electronic coupling than are those of β symmetry. We have assigned bands I and II in the monometallic complexes as MLCT transitions involving the LUMOs of α and β symmetry (α higher energy only for the dpp complexes). These bands are roughly comparable in intensity, and this implies roughly comparable metal−ligand mixing ($H_{ML}(I) \sim H_{ML}(II)$), and this is reasonably consistent with the significant orbital contributions calculated at the pyrazine nitrogen atoms in both symmetries (Figure 3). As a consequence, simple superexchange arguments[73,74,87] would imply roughly comparable metal−metal mixing. However, in the α symmetry the N-atom orbital phases are symmetrically related (with respect to a C_2 axis perpendicular to the pyrazine moiety), while in the β symmetry they are antisymmetrically related. Thus, the orbitals of two metals coupled by means of a π^* orbital with β symmetry would be expected to be out of phase, and this might result in very little metal−metal mixing. This is reminiscent of the bridging ligand phase effects observed in cyanide-bridged complexes.[26,28]

C.5. Optical/Electrochemical Comparison. We have observed much larger values of $(h\nu_{max} - F\Delta E_{1/2})$ for the dpp-bridged dimers than for the monomers (Table 3 and Figure 4). Arguments presented above demonstrate that this difference cannot be attributed to a large difference in reorganizational energies. Observations, such as the very similar values of ν_{NH} for monometallic and bimetallic tetraammine complexes, are consistent with very little difference in electron delocalization in the ground state. The band I energies of the bimetallic complexes do not vary in proportion to variations in $E_{1/2}(Ru^{III}|Ru^{II})$. There are several, not necessarily exclusive, possible interpretations of this behavior: (1) the stabilization energy contributions, ϵ_s, that result from metal−ligand mixing enter differently into the transition energy for monometallic and bimetallic complexes, (2) the observed transition is not properly classified as an MLCT transition,[65] or (3) the optical excitation involves a metal HOMO different from that accessed electrochemically. The first possibility is the most straightforward. The shift of the ground-state PE minimum ($\alpha_{ML}{}^2x_0$) in the monometallic complexes compensates partly for the effects of ground-state stabilization and vertical excited-state destabilization, $\epsilon_d{}^v$, while in the dimer there should be little shift of the ground-state PE minimum (Figure 10). In terms of the arguments above, the absorption of the symmetric dimer should occur at approximately $[\lambda_{reorg}{}^{o}(4\alpha_{ML}{}^2) + 2.8\epsilon_{ML} - H_{MM'}(1 - 4\alpha_{ML}{}^2)]$ higher energy than the monomer (relative to the values of $F\Delta E_{1/2}$). Values of $H_{ML}{}^2/E_{ML} \cong \epsilon_s \cong \epsilon_d \cong 2.5 \times 10^3$ cm^{-1} for ammine complexes are reasonably consistent with the implications of the MLCT absorption/emission properties discussed above. Pyrazine-bridged bimetallic Os complexes have been reported to have similar values of $(h\nu_{max} - F\Delta E_{1/2})$.[37]

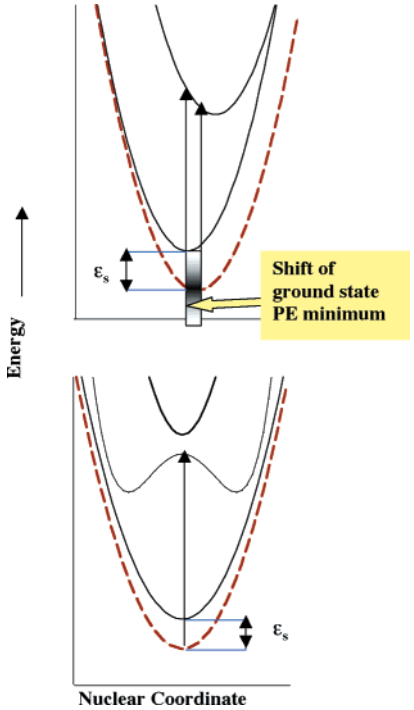

Figure 10. Illustration of the effects on the ground state of mixing with one (top) and two degenerate-coupled (bottom) excited states. For mixing with a single excited state, the shift of the ground-state PE minimum partially compensates for the effects of ground-state stabilization. With two degenerate excited states, the ground-state PE minimum does not shift and ϵ_s contributes more strongly to $h\nu_{max}$.

We believe that the other two possibilities are less likely. The amount electron density delocalized seems small enough that the MLCT classification is still useful in the dimers. It is unlikely that the electrochemical oxidations access markedly different metal HOMOs in the monomers and the dimers.

Conclusions

Overall, our observations indicate that there is appreciable charge delocalization in Ru^{II}−polypyridyl complexes and that this has some striking effects on the trends in the properties of these complexes. The bandwidth of the lowest energy MLCT absorption of $[Ru(NH_3)_4bpy]^{2+}$ implies about 10%

(88) Swayambunathan, V.; Endicott, J. F. Work in progress.

delocalization of electron density between metal and ligand, provided the distribution of solvent environments does not affect the bandwidth in a manner different from its effect on the reorganizational energy. The fraction of electron density delocalized is similar, but probably slightly larger (10−40%), in the dpp analogue. Electron exchange energy does appear to play a role in these systems, more in the dpp than in the bpy complexes. The lowest energy MLCT excited states of $[Ru(bpy)_2(dpp)]^{2+}$ and $[Ru(NH_3)_4(dpp)]^{2+}$ complexes populate the β-LUMO rather than the more commonly expected α-LUMO. This means that the lowest energy π^* orbital of dpp differs in symmetry from that of the parent pyrazine ring, and this feature is unique to the dpp ligand in the series considered. Similarly, the ligand reductions of the dpp complexes predominately involve the β-LUMO, and this readily accounts for the previously observed deviations of the electrochemical reductions of dpp complexes from a correlation with bond order,[9] since the β-LUMOs mix more strongly with the pyridyl moieties than do the α-LUMOs. The α-LUMOs would be involved in ligand reductions of all but the dpp complexes.

Spectroscopic, electrochemical, and computational observations on a series of Ru^{II}−polypyridyl complexes have led to the following conclusions.

1. The LUMO and LUMO + 1 of dpp, bpy ligands, and closely related ligands are not greatly different in energy.

2. The changes in electron exchange contributions that result from configurational mixing are smaller than the stabilization energies associated with electron delocalization. The fraction of electrons delocalized seems to be similar in bpy and dpp complexes that differ only in these ligands, but the exchange contribution appears to be significantly larger for complexes with dpp ligands.

3. The MLCT excited-state spectra of dpp-bridged complexes can be complicated by large "intervalence" splittings mediated by one, but not both, of the lowest energy π^* orbitals. This difference in mediation of Ru^{II}/Ru^{III} coupling suggests a bridging ligand orbital phase effect on the superexchange coupling.

4. The connection between the different species involved in the electrochemical and photochemical processes can be made by means of an electron-transfer equilibrium constant, K_{DA}, and the contributions to K_{DA} can assessed in terms of perturbation theory based arguments.

Acknowledgment. The authors thank the Office of Basic Energy Sciences of the Department of Energy for partial support of this research. We thank Professor Karen Brewer for access to preparative details for the dpb and dpq complexes. We have profited from an extensive exchange with Professor A. B. P. Lever regarding the interpretation of many issues raised in this study.

Supporting Information Available: Table of elemental analyses, description of synthesis of complexes, figure of spectral assignments for $[Ru(NH_3)_4bpy]^{2+}$, ambient emission spectra of $[Ru(NH_3)_2(bpy)_2]^{2+}$ and $[Ru(bpy)_3]^{2+}$, figure comparing IPCT transition energies to electron-transfer parameters, paragraph describing exchange energy contributions, paragraph describing perturbation theory stabilization energies, paragraph describing the extraction of reorganizational energies from bandwidths, and figure relating N−H stretching frequencies to variations in MLCT energies. This material is available free of charge via the Internet at http://pubs.acs.org.

IC010172C